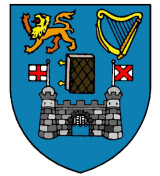




**Erasmus Mundus**



Education and Culture



TRINITY COLLEGE  
DUBLIN

## **ERASMUS MUNDUS MASTER OF MECHANICAL ENGINEERING**

### **MEMOIRE- THESIS**

### **AUTHOR**

**Venu Gopal GORU**

### **TITLE**

**Analysis of the Potential of DynaFlexPro  
as a Modeling Software by its  
Application in the Roll Stability of Heavy-Duty Elliptical Tankers using  
Trammel Pendulum to Simulate Fluid Sloshing.**

**June 2007**

INSTITUT NATIONAL DES SCIENCES APPLIQUEES DE LYON - FRANCE  
SCOLA TECHNICA SUPERIOR D'ENGINYERIA INDUSTRIAL DE BARCELONA DE LA  
UNIVERSITAT POLITECNICA DE CATALUNYA - ESPAGNE  
THE COLLEGE OF THE HOLY AND UNDIVIDED TRINITY OF QUEEN ELIZABETH NEAR DUBLIN -  
IRLANDE

## ABSTRACT

One of the most common ways for commercial vehicles to lose their stability is by rollover. Partially filled heavy-duty tankers manoeuvring constant radius turns or lane change maneuvers have lower rollover threshold than other vehicles because of the high center of gravity and dynamic sloshing of the liquid payload. A number of analytical and numerical methods have been used till date to study the motion of fluid in a container and its effect on the container. One of the simplest and most effective ways is by modeling the fluid as a pendulum. Depending on the shape and size of the container, different types of pendulums have been proposed. In this case as the study was based on elliptical cisterns, a trammel pendulum was chosen and the fundamental basis of selecting the appropriate pendulum parameters has been obtained by studies performed by Salem [12].

One of the main aspects of this project is the utilization of completely new multibody computer-aided engineering (MCAE) software packages called *DynaFlexPro (DFP)* and *DynaFlexPro/Tire* released in 2005 by MotionPro, Inc and marketed by MapleSoft Inc. These new commercial packages of Maple were chosen to model the Trammel pendulum and the Tractor and articulated Tanker vehicle.

Firstly a model of a trammel pendulum was created and its kinematic and dynamic effects were studied. The fundamental basis of selecting the appropriate pendulum parameters have been obtained by matching the pendulum dynamic effects with fluid sloshing dynamic effects obtained by using Finite Element (FE) fluid models in the work of Salem. Once a working model was achieved, a 2-D Tanker model was made and the Trammel pendulum model was integrated to study the effect of sloshing on the roll stability of heavy duty tankers. The rollover threshold of 2-D models ranged from 0.9g to 0.25g because of which more realistic 3-D models of Tractor and Tanker were made. Due to some problems in the assembly of Tractor and Tanker, the 3-D Tanker was modified and basic tests were simulated. The 3-D Tanker model predicted critical fill

levels that agree with the values reported in the literature based on much more complex and time consuming experimental and analytical methods proving the efficiency of the modeling software. In addition sloshing effects were clearly visible from the results validating the trammel pendulum as a simple and efficient way of modeling sloshing of fluids in elliptical tankers.

# Acknowledgements

*I wish to express my sincere gratitude to Prof. Philippe Lonjou of the Department of Génie Mécanique, INSA, Lyon for his constant inspiration, guidance and personal attention while carrying out the project work. I am indebted to him for extending all the necessary facilities, information, guidance and constant support during the course of project and thesis preparation.*

*I would also like to thank Prof. Henry Rice of the Department of Mechanical and Manufacturing Engineering, Trinity College, Dublin for his support and guidance last year and for this keen interest in the initiation of the project.*

*Thanks are also due to Centre d'Intéret Dynamique de la Locomotion et de Conception Mécanique for their support of this study and for the environment and equipment they have provided throughout this research. Special thanks to Mr. L. Maiffredy and Mr. J.P. Brossard for sharing their immense knowledge without which it would have been impossible to realize this project.*

**Venu Gopal GORU**

**EMMME**

# Table of Contents

<b>Abstract</b>	<b>2</b>
<b>Acknowledgements</b>	<b>4</b>
<b>Table of Contents</b>	<b>5</b>
<b>List of Figures</b>	<b>7</b>
<b>Chapter 1: Introduction and Literature Review</b>	<b>10</b>
1.1 Rollover of Heavy Vehicles	11
1.2 The Case for Articulated Vehicles	13
1.3 Heavy Duty Articulated Tankers	14
1.4 Fluid-Container Interaction	15
1.5 Fluid-Vehicle Interaction	19
1.6 Aims and Objectives	25
<b>Chapter 2: Modeling of the fluid in Elliptical containers</b>	
<b>by Trammel Pendulum</b>	<b>26</b>
2.1 Sloshing in Elliptical Tanks	26
2.2 Mathematical Modeling of Sloshing in Elliptical Tanks	27
2.3 Trammel Pendulum Parameters	31
2.4 <i>DynaFlexPro</i> Trammel Pendulum Model	33
2.5 Simulation and Results	36
<b>Chapter 3: Vehicle Models and Simulation</b>	<b>40</b>
3.1 Introduction to <i>DynaFlexPro/Tire</i>	40
3.2 2-D Model	46
3.3 Modelization of the Trailer	55
3.4 Tractor 3-D Model	58
3.5 Problems with assembly of Tractor and Trailer	62
3.6 Simplified Model – Trailer with Trammel Pendulum	63

<b>Chapter 4: Conclusions and Discussion</b>	<b>70</b>
<b>Chapter 5: Recommendations and Future Work</b>	<b>74</b>
<b>References</b>	<b>76</b>
<b>Appendix</b>	<b>78</b>

## List of Figures

Figure 1.1.1: Rollover of a Tractor Trailer during a manoeuvre.

Figure 1.4.1- Equivalent mechanical model for a partially filled ellipsoidal tank and the associated variation of sloshing frequencies with liquid depth Rattayya (1965).

Figure 1.5.1.1: Two positions of the liquid during a steady state turning

Figure 1.5.1.2: Sloshing of the liquid during breaking

Figure 1.5.1.3: Rollover threshold in a steady turn as a function of the percentage of load of unrestrained liquid and tank shapes (adapted from Strandberg, 1978).

Figure 1.5.1.4: Rollover threshold in a transient turn as a function of the percentage of load of unrestrained liquid and tank shapes (adapted from Strandberg, 1978).

Figure 2.2.1: Steady State Motion of the Liquid Cargo under Vehicle Roll and Lateral Acceleration of an Elliptical Cross-section [9].

Figure 2.2.2: Locus of C.G. location for a given volume of fluid in an elliptical container

Figure 2.2.3: C.G. of fluid volume contour drawn by an elliptical trammel mechanism.

Figure 2.2.4: Diagram showing the fill level in an elliptical tanker.

Figure 2.3.1:  $\bar{b}/b$  vs fill level for different values of  $a/b$

Figure 2.3.2:  $M_p/M_t$  vs fill level for different values of  $a/b$

Figure 2.3.3:  $h_o/b$  vs fill level for different values of  $a/b$

Figure 2.4.1: Trammel Pendulum

Figure 2.4.2: *DynaFlexPro* model of Trammel Pendulum.

Figure 2.5.1: Position and Velocity of Pendulum angle at 5 deg initial angle

Figure 2.5.2: Position and Velocity of Pendulum angle at 30 deg initial angle

Figure 2.5.3: Position and Velocity of Pendulum angle at 60 deg initial angle

Figure 2.5.4: Position and Velocity of Pendulum angle at 90 deg initial angle

Figure 2.5.5: Position and Velocity of Pendulum angle at 150 deg initial angle

Figure 2.5.6: Natural Frequency vs fill level for 5 degree initial angle

Figure 2.5.7: Natural frequency vs. fill level for a fluid volume in an elliptical tank with different values of  $a/b$  at initial fluid surface angle = 5 degrees obtained using FEM by Salem.

Figure 3.1.1: Tanker used for modeling.

Figure 3.1.2: Main dimensions of the Tractor.

Figure 3.1.3: Main dimensions of the Trailer.

Figure 3.1.4: Design of highways by clothoid curve (left) and a simple clothoid curve (right).

Figure 3.1.5: Lane Change Manoeuvre.

Figure 3.2.1: 2-D Roll model of the Tanker

Figure 3.2.2: *DynaFlexPro* model for 2-D model.

Figure 3.2.3: Lateral Acceleration vs time for a Clothoid test

Figure 3.2.4: Lateral Acceleration vs time for a Lane Change Manoeuvre.

Figure 3.2.5: Vertical displacement of center of left tire with respect to ground for a 50% fill level during a Clothoid Test.

Figure 3.2.6: Pendulum angle vs time for a 50 % fill level during a Clothoid Test.

Figure 3.2.7: Change of roll angle vs time for a 50% fill level during clothoid test.

Figure 3.2.8: Plot of lateral acceleration vs fill level for a Clothoid test.

Figure 3.2.9: Vertical displacement of center of left tire during a Lane Change manoeuvre.

Figure 3.2.10: Change of roll angle vs time during a Lane Change Manoeuvre.

Figure 3.2.11: Change of Pendulum angle vs time during a Lane Change Manoeuvre.

Figure 3.2.12: Plot of Lateral Acceleration vs Fill Level for Lane Change Manoeuvre.

Figure 3.3.1: A 3 dimensional picture of the simplified Tanker modeled showing the coordinate system used.

Figure 3.3.2: The *DynaFlexPro* model for the Tanker coupled with the Trammel pendulum.

Figure 3.4.1: A 3 dimensional model of the simplified Tractor showing the coordinate system used.

Figure 3.4.2: The *DynaFlexPro* of the Tractor

Figure 3.6.1: Vertical displacement of the point of articulation with the Tanker for a clothoid test at 72 km/hr.

Figure 3.6.2: The *DynaFlexPro* of the Tanker with the Driver model attached.

Figure 3.6.3: Vertical displacement of the center of tire with respect to the ground during a clothoid test at 50% fill level.



Figure 3.6.4: Lateral Acceleration during a clothoid test at 50% fill level.

Figure 3.6.5: Roll angle during a clothoid test at 50% fill level.

Figure 3.6.6: Trajectory of driver during a clothoid test at 72 km/hr.

Figure 3.6.7: Lateral Acceleration vs fill level for a clothoid test at 72 km/hr.

# **CHAPTER ONE**

## **INTRODUCTION AND LITERATURE REVIEW**

The aim of this research study can be grouped into two main parts. Firstly, explore the capacities of *DynaFlexPro* as a modeling software. Second, to study the roll stability of heavy-duty Tankers using trammel pendulum to simulate fluid sloshing. First a literature review was conducted to collect all the information necessary to approach the problem and know all the governing factors and parameters regarding heavy-duty vehicle stability and fluid sloshing. This is the main content of the first chapter. Basic study regarding the rollover of heavy vehicles specifically regarding vehicles carrying liquid load was done. Also the study related to sloshing of liquids and its interaction with containers and impact on vehicle stability can be found in this chapter. The chapter ends with the breakdown of the aims and objectives of this research project.

The second chapter deals with the mathematical modeling and simulation of the trammel pendulum. The criterion of choosing the trammel pendulum model has been shown here. The fundamental basis of selecting the appropriate pendulum parameters have been obtained by studies performed by Salem [12]. Once the parameters of trammel pendulum were found simulations were done by the models created in *DynaFlexPro* to verify the pendulum characteristics.

Once the trammel pendulum was developed, vehicle models were developed and trammel pendulum was integrated with it. A number of models were created to simulate the vehicle characteristics during two basic manoeuvres – turning around a clothoid and lane change manoeuvre. Chapter three relates the creation of 2-D and 3-D models and the simulation performed. The results found from chapter three are discussed in the following chapter of Conclusions and Discussion. It also deals with the advantages and features of *DynaFlexPro* when compared to other softwares.

The report ends with the recommendations to the reader regarding the software and the models created. Certain tips and advices have been given which should be implemented to carry this study further and improve the results.

## 1.1 Rollover of Heavy Vehicles

The roll-over of heavy vehicles is an important road safety problem world-wide. Several studies have reported that a significant proportion of the serious heavy vehicle accidents involve roll-over. Rollover accidents of commercial vehicles are especially violent and cause greater damage and injury than other accidents. The relatively low roll stability of commercial trucks promotes rollover and contributes to the number of truck accidents.

There are over 15,000 rollovers of commercial trucks each year in the U.S. That is about one for every million miles of truck travel. About 9,400 of these—about one for every four million miles—are rollovers of tractor-semi trailers. In the UK during the year 1993, 545 heavy vehicles were involved in roll-over accidents [1]. Roll-over accidents accounted for 6% of all accidents to articulated heavy vehicles and 30% of accidents to heavy vehicles at roundabouts.

Commercial truck rollover is strongly associated with severe injury and fatalities in highway accidents. About 4 percent of all truck accidents involve rollover, but more than 12 percent of fatalities in truck accidents involve rollover (General Estimates System, 1995 and *Truck and Bus Crash Fact Book*, 1995)[1].

The association of rollover with injuries to the truck driver is even stronger. While only 4.4 percent of tractor-semitrailer accidents are rollovers, 58 percent of the fatal injuries to the truck driver occurred in rollover crashes (General Estimates System and *Trucks Involved In Fatal Accidents*, 1992–1996). Rollover is overrepresented in all forms of truck-driver injury and that the level of overrepresentation increases progressively with the severity of injury.

Heavy freight vehicles have poor rollover limits and are thus prone to the rollover accidents. Under normal road conditions the heavy freight vehicle lateral skid would probably not be initialized before the vehicle rolls over. For example, a survey of highway accidents involving heavy freight vehicles in Canada revealed that nearly 77% of rollover accidents occurred on dry pavement and could be classified as manoeuvre-induced rollovers.

A manoeuvre-induced rollover is primarily attributed to the dynamic roll behavior of the vehicle, while the contributions from the tripping mechanism are absent. This kind of rollover may occur during low-speed cornering and braking or high-speed evasive directional manoeuvres.



Figure 1.1.1: Rollover of a Tractor Trailer during a manoeuvre.

*It is clear that even a modest increase in roll stability can lead to a significant reduction in the frequency of roll-over accidents.* This provides a compelling motivation for research into improving roll stability of heavy vehicles because of the serious safety, cost and environmental implications of roll-over accidents.

## 1.2 The case for articulated vehicles:

The use of long articulated vehicles is economically attractive due to lower fuel and driver costs per tonne of cargo. However it has been shown that poorly designed multiple unit vehicles can suffer from dangerous roll and handling instabilities. For this reason, government regulators have traditionally been hesitant to sanction the use of such vehicles.

McFarlane et al. proposed performance measures to guide regulators assessing the safety of novel long combination vehicles [11]. They suggested that vehicle safety could be assessed with some confidence by considering two key performance indicators:

- *Rearward amplification* (that is, the ratio of the lateral acceleration of a trailing unit of a combination vehicle to the lateral acceleration of the leading unit, in response to a sinusoidally varying steering input); and
- *Steady-state roll stability*.

There are few accident statistics available for long combination vehicles so it is not yet possible to demonstrate a robust statistical correlation between these proposed indicators and the frequency of roll-over accidents. However the authors noted a parallel with the aircraft industry where accidents are rare but the use of performance-based standards is widespread.

McFarlane suggested that governments should consider a flexible, performance based approach to the regulation of multiple unit vehicles and detailed the potential economic benefits. Woodrooffe documented the history of heavy vehicle regulation in the Canadian province of Saskatchewan through the 1980s and 1990s.

Several novel long combination vehicles that had previously been prohibited were permitted to operate on selected routes, and no serious accidents were reported. Lobbied by fleet operators, regulators are demonstrating an increasing flexibility towards allowing longer combination vehicles to operate on major highways and motorways, providing the vehicles satisfy stringent roll stability and handling performance criteria.

### **1.3 Heavy duty articulated tankers**

In the majority of commercial truck operations, the load on the vehicle is fixed and nominally centered. In certain cases, however, the load may be able to move in the vehicle, with the potential of affecting the turning and rollover performance. The most common examples of moving loads are bulk, liquid tankers with partially filled compartments; refrigerated vans hauling suspended meat carcasses; and livestock. The performance properties of commercial vehicles used in these applications may be influenced by the free movement of the load in either longitudinal or lateral directions. This section presents material on the first type of load.

#### **Liquid Loads**

Heavy-duty tanker trucks carrying liquid cargo have poor overturning and skidding stability because of the high center of gravity and sloshing of the liquid. The problem of instability is further exacerbated when the trailer is subjected to various dynamic manoeuvres, such as lane change, u-turns and braking in a turn or cornering. Roll over instability is particularly sensitive to the dynamic sloshing effects in partially filled tanks. Lack of lateral force feedback from the trailer further reduces the overall safety. Thus, these two conditions namely, high center of gravity and the dynamic sloshing of the liquid cargo have placed heavy-duty tanker trucks in a very high-risk category on the roadways.

In the operation of a bulk-liquid transport vehicle, the moving load that can affect its cornering and rollover behavior is the presence of unrestrained liquid due to a partially filled tank or compartment. A compartment that is filled to anything less than its full capacity allows the liquid to move from side to side, producing a “slosh” load condition. Slosh is of potential safety concern because the lateral shift of the load reduces the vehicle’s performance in cornering and rollover, and the dynamic motions of the load may occur out of phase with the vehicle’s lateral motions in such a way as to become exaggerated and thus further reduce the rollover threshold. The motions of liquids in a tank vehicle can be quite complex due to the dependence of the motions on tank size and

geometry, the mass and viscosity of the moving liquid, and the manoeuvre being performed (Dalzell, 1967; Komatsu, 1987; and Krupka, 1985). Fundamental analyses of sloshing liquids in road tankers appeared in the literature from the 1970s. A number of more elaborate computer studies arose in the late 1980s and early 1990s. This discussion is constrained to basic elements that provide insight on the mechanisms by which fluid motions influence rollover. The mechanisms of slosh are most readily described in simple steady-state cornering, although it is in transient manoeuvres that the most exaggerated fluid displacements take place.

## 1.4 Fluid Container Interaction

A number of analytical and numerical methods have used till date to study the effect of sloshing and modelize it. Rayleigh (1876) was the first who tackled the problem of fluid sloshing in partially filled containers. Rayleigh used a pendulum to simulate the dynamic effects of sloshing and obtained the correct lengths for regular pendulums that matched the fluid natural frequencies. Lamb (1945) was the first to analytically obtain the transverse mode fundamental frequency  $\omega_n$  of a 50% filled horizontal cylindrical tank of diameter D, which was given by:

$$\omega_n = 1.169\sqrt{g/D} \quad (2.2.1)$$

After the advent of the aerodynamics industry in the 50's and 60's much more research followed by Graham and Rodriguez (1952). They simulated the motion in rectangular tank surface by a fixed mass and a rotary inertia. Bauer (1958 A) studied the inertia of a fluid in completely filled circular cylindrical tank and compared the moment of inertia of an ideal fluid (incompressible and nonviscous) with the moment of inertia of the same fluid in a frozen state. He found out that they can be considerably different. Bauer (1958 B) also found out that the moment of inertia of a liquid in a partially filled tank is strongly frequency dependant and that it is different from the moment of the same amount of fluid in a frozen state. Also, Bauer (1958C) studied the effect of damping on

fluid inertia in a partially filled circular tank and found that the damping effect on the calculated inertia is negligible at high levels of fill.

Budiansky (1960) estimated the natural frequencies, mode shapes, and forces exerted on the walls of a partially filled circular canal and spherical tanks due to lateral excitation resulting in small-amplitude oscillations of the fluid. Budiansky considered the antisymmetric modes only since the symmetrical modes would not be induced by transverse motion of the tank. He also assumed an irrotational inviscid fluid, which is a good approximation for a deep container. Budiansky carried out the analysis using an arbitrary velocity potential on the surface and solving the continuity and the linearized Bernoulli equation to obtain homogeneous Fredholm integral equation describing the surface fluid motion.

Rattayya (1965) evaluated the natural frequencies and mode shapes of a fluid in a partially filled ellipsoidal tank. He also simulated the first two modes of fluid vibration using a fixed mass and two laterally vibrating masses on springs. Figure 1.4.1 below shows the equivalent mechanical model and the associated chart used to find the parameters of this model. It can be seen that the first two natural frequencies of the fluid sloshing reach infinity at all tank aspect ratios when the level of fill approaches the complete full condition.



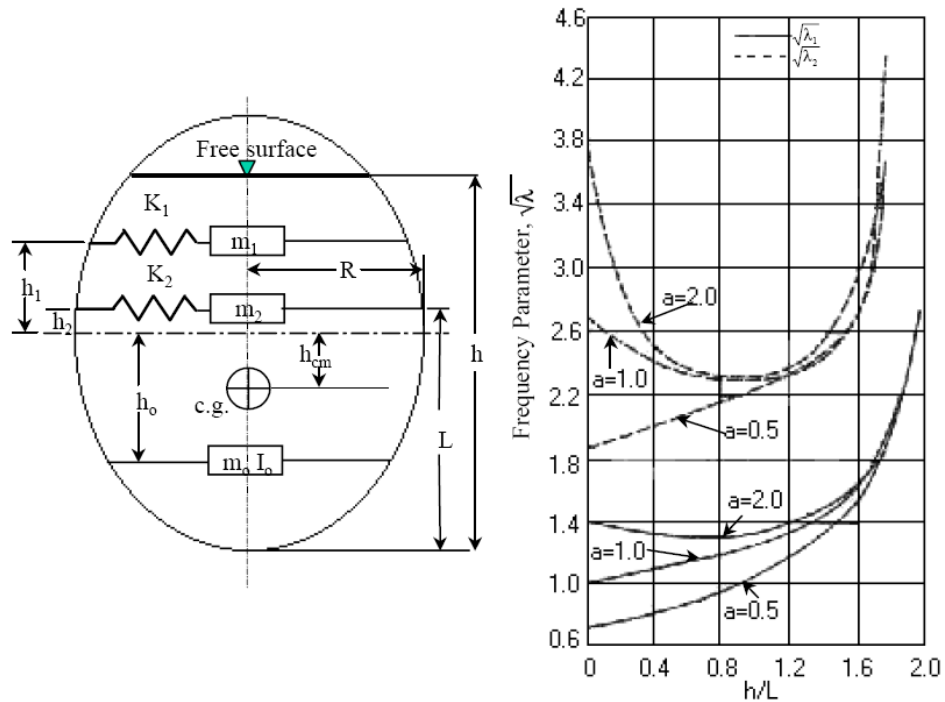


Figure 1.4.1- Equivalent mechanical model for a partially filled ellipsoidal tank and the associated variation of sloshing frequencies with liquid depth Rattayya (1965).

The parameter  $\lambda = \frac{\omega_n^2 R}{g}$  on the vertical axis is the frequency parameter.

"a" is the ratio  $L/R$ , "g" is the gravitational acceleration, "R" is the tank radius as shown in Figure 1.4.1, and  $\omega_n$  is the n'th natural frequency of the fluid lateral slosh.

Sankar et. al (1992 A) considered the non-linearities of fluid sloshing in an elliptical container. Sankar stated that all the theories used before to investigate the fluid sloshing were linear theories and they are in good agreement with the experiments, but only over a small range of motion amplitude. They mentioned many parameters that are commonly used, and gave ranges of these parameters which if exceeded, the nonlinear effects can not be neglected. One of the most important parameters is the lateral acceleration which should not exceed 0.2 g for fill levels of about 50% for a close to circular cross section tank. They solved the following sets of equations to determine the non-linear fluid behavior in an elliptical tank:

Navier-Stokes equations for an incompressible fluid in 2-D:

$$St \frac{\partial U}{\partial T} + \frac{\partial U^2}{\partial X} + \frac{\partial UV}{\partial Y} = \frac{G_x}{Fr} - Eu \frac{\partial P}{\partial X} + \frac{1}{Re} \nabla^2 U$$

$$St \frac{\partial V}{\partial T} + \frac{\partial UV}{\partial X} + \frac{\partial V^2}{\partial Y} = \frac{G_y}{Fr} - Eu \frac{\partial P}{\partial Y} + \frac{1}{Re} \nabla^2 V$$

The continuity equation:

$$\frac{\partial U}{\partial X} + \frac{\partial V}{\partial Y} = 0$$

Popov et. al, (1993 B) studied the dynamics of liquid sloshing in baffled and compartmented rectangular road containers during uniform braking and steady state cornering. The influence of the number of separating walls, size and location of orifices in the separating walls was studied. The transient response of the fluid was obtained by numerically solving 2-D Navier-Stokes, continuity, and free surface equation using the modified Marker-and-Cell technique described in details by Popov (1991). The braking or acceleration manoeuver was presented by a constant change in deceleration or acceleration. This approach was proved to be valid by Popov et. al 1992).

Popov et. al, (1993 C) conducted a study to obtain the optimal shape of a rectangular road container. They integrated the static momentum equations of a fluid in 2-D to obtain the objective function represented by the overturning moment around the middle point of the container. The objective function was minimized with respect to the container height and fill level, considering the lateral acceleration as a parameter.

The following table gives some reduced formulas to evaluate the fundamental lateral natural frequency of vibration in a half-full cylindrical tank. The last row gives the result of a finite element fluid model [12]. It can be seen that Bohn reduced formula for the fundamental natural frequency of lateral fluid sloshing in a half full cylindrical tank is biased towards a higher value of natural frequency from any other method (at least 30% higher from the closest method). Thus the result obtained by Bohn is questionable.

Model or Method to Obtain The Fundamental natural Frequency In a Half Full Cylindrical Tank	Formula
Rayleigh (1876)	$\omega_n = 1.1644\sqrt{\frac{g}{R}}$
Lamb (1945)	$\omega_n = 0.8266\sqrt{\frac{g}{R}}$
Budiansky (1960)	$\omega_n = 1.169\sqrt{\frac{g}{R}}$
<b>Bohn (1981)</b>	$\omega_n = 1.535\sqrt{\frac{g}{R}}$
WVU LS-Dyna 3D Fluid Model	$\omega_n = 1.1\sqrt{\frac{g}{R}}$

Table 1.4.1– Reduced formulas to evaluate the fundamental lateral natural frequency of vibration in a half-full cylindrical tank.

## 1.5 Fluid-Vehicle Interaction

### 1.5.1 Sloshing During Turning

#### *Steady Turning*

When a slosh-loaded tanker performs a steady-state turn, the liquid responds to lateral acceleration by displacing laterally, keeping its free surface perpendicular to the combined forces of gravity and lateral acceleration.

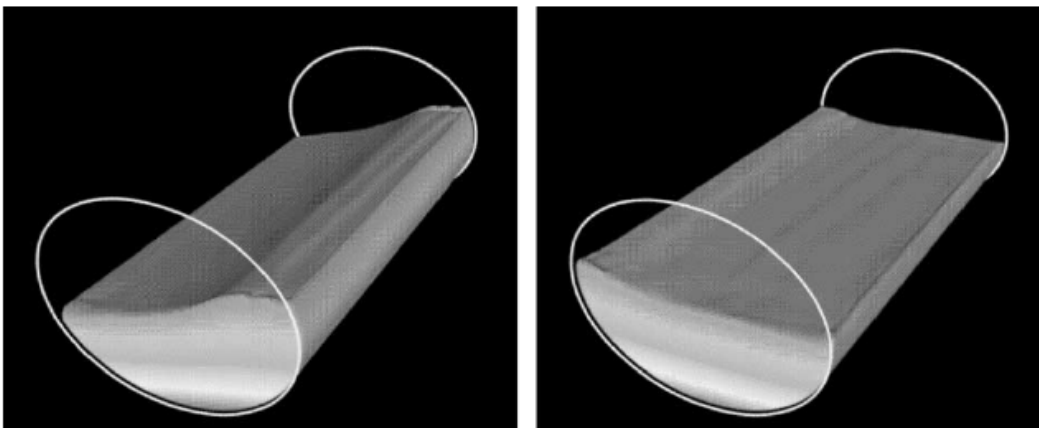


Figure 1.5.1.1: Two positions of the liquid during a steady state turning

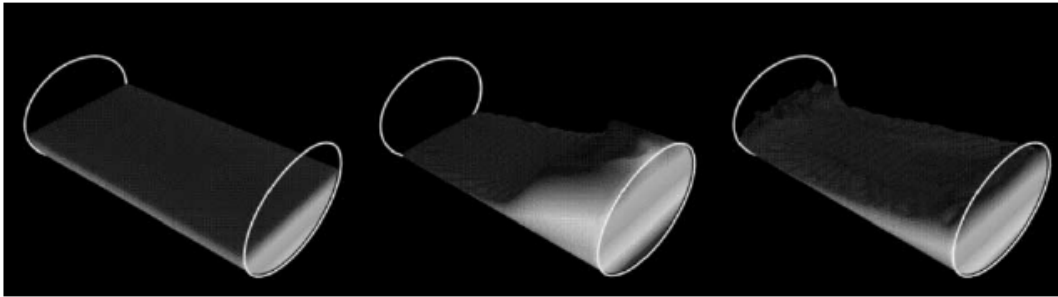


Figure 1.5.1.2: Sloshing of the liquid during braking

The mass center of the liquid moves on an arc, the center of which is at the center of the circular tank. In effect, the shift of the liquid produces forces on the vehicle as if the mass of the load were located at the center of the tank.

With more complex tank shapes, even the steady-state behavior becomes somewhat difficult to analyze. In particular, with unusual tank shapes it becomes more difficult to describe the motion of the liquid's center of mass as a function of lateral acceleration. At low lateral accelerations, the liquid movement is primarily lateral, centered at a point well above the tank center. Hence, its effect is similar to having a very high mass center. With increasing lateral acceleration, the mass center follows a somewhat elliptical path. While the circular tank results in a vehicle with a higher load center, efforts to reduce the load height by widening and flattening the tank can be expected to increase vehicle sensitivity to slosh degradation of the rollover threshold.

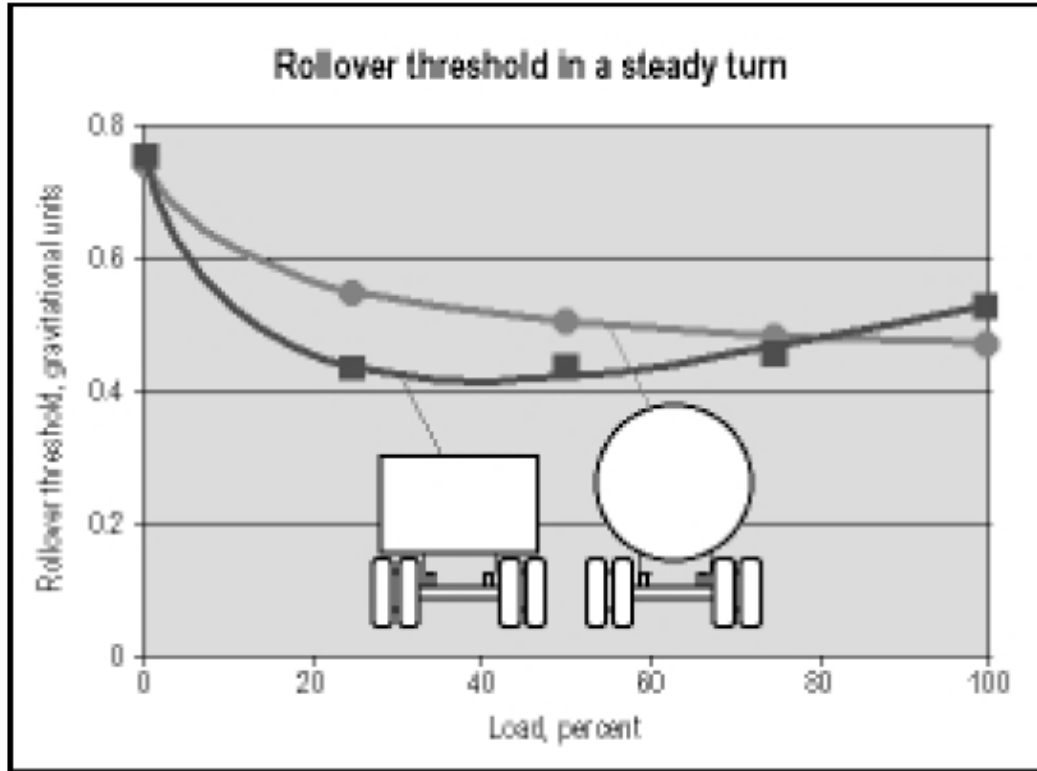


Figure 1.5.1.3: Rollover threshold in a steady turn as a function of the percentage of load of unrestrained liquid and tank shapes (adapted from Strandberg, 1978).

The effect is illustrated by the plot in figure 1.5.1.3 [14] which is adapted from data by Strandberg (Ranganathan later presented very similar results). The figure shows rollover threshold versus load condition in steady-state cornering. For a circular tank, increasing load lowers the threshold continuously due to the increasing mass of fluid free to move sideways. In this case, the minimum rollover threshold occurs at full load. For a vehicle with a modified rectangular tank, higher levels of rollover threshold occur when the tank is either empty or full, although at intermediate load conditions the rollover threshold is severely depressed due to the greater degree of lateral motion possible for the unrestrained liquid. Thus, the rectangular tank shape (in contrast to the circular) can potentially result in rollover thresholds with sloshing loads that are less than that of the fully loaded vehicle.

### ***Transient Turning***

In transient manoeuvres such as an abrupt evasive steering manoeuver (e.g., a rapid lane change), slosh loads introduce the added dimension of dynamic effects. With a sudden steering input, the rapid imposition of lateral acceleration may cause the fluid to displace to one side with an underdamped (overshooting) type of behavior. The difference between the steady-state and transient manoeuvres is primarily a matter of the time involved in entering the turn. The steady-state type of behavior is observed when the turn is entered very slowly, whereas the transient behavior applies to a very rapid turning manoeuver. The response of the liquid mass to a step input of acceleration would be seen to be displaced to an amplitude of approximately twice the level of the steady-state amplitude.

In a lane-change manoeuver in which the acceleration goes first in one direction and then the other, even more exaggerated response amplitude can be produced. In general, the degree to which the dynamic mode is excited depends on the timing of the manoeuver. The unrestrained liquid will have a natural frequency for its lateral oscillation which depends on the liquid level and cross-sectional size of the tank. As for dynamic systems in general, if the frequency content of input (lateral acceleration) stays below this natural frequency, the response is largely quasi-static, but if the input contains substantial power at or above the natural frequency, the response will be dynamic. Indeed, the two-second lane change used as a typical evasive manoeuver for evaluating rearward amplification constitutes a lateral acceleration input at just that frequency closely matched to the slosh frequency. Hence it must be concluded that dynamic slosh motions can be readily excited on a tanker of normal size, especially in the course of evasive manoeuvres such as a lane change. In transient manoeuvres, rollover thresholds are depressed by this dynamic motion.

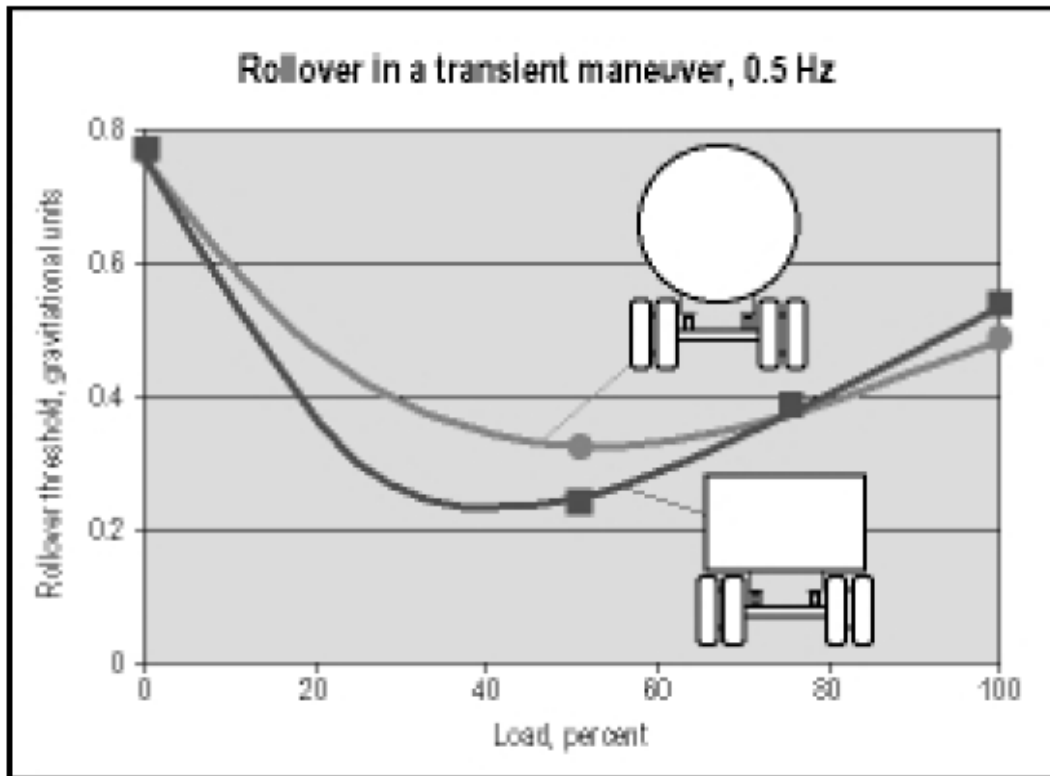


Figure 1.5.1.4: Rollover threshold in a transient turn as a function of the percentage of load of unrestrained liquid and tank shapes (adapted from Strandberg, 1978).

Figure 1.5.1.4 shows the estimated rollover threshold as a function of load for unrestrained liquids in a transient manoeuvre, which is adapted from data presented by Strandberg. In the transient case, even the circular tank experiences reduced rollover thresholds when partially loaded because the fluid can “overshoot” the steady-state level. Understandably, the elliptical tanker is even worse. Though the results shown are derived from analytical studies, experimental tests of partially loaded tankers generally confirm these observations (Culley et al., 1978).

### ***Partial Liquid Loads***

A number of times vehicles have to run with partial loads. This is especially true with local delivery tankers hauling gasoline and home-heating fuel. The question is: What can be done to reduce the sensitivity and hence the potential risks of using these vehicles, once a substantial fraction of their load has been delivered? Of course, specifying a vehicle with suspension systems most resistant to rollover is a first step. However, at least two other aids are available:

***Baffles:*** Baffles are commonly used in tank vehicles, except in special cases where provisions for cleaning prevent their use (such as bulk-milk haulers). However, the common baffle arrangement is a transverse baffle intended to impede fore/aft movement of the load. These transverse baffles have virtually no utility in preventing the lateral slosh influential to roll stability. To improve roll performance, longitudinal baffles would be required, but design and cost considerations have practically eliminated their use.

***Compartmentalization:*** A more common method for improving cornering performance with tankers under partial loading conditions is to subdivide the tank into separate compartments. Ideally, the compartments are completely emptied on an individual basis at a drop spot so the vehicle is never subject to a sloshing load. The only precaution in this type of use is that the delivery route should be planned to empty from the rear of the vehicle first. When it is not possible to completely empty each compartment, a reduced slosh sensitivity exists, but is often not significant as long as only a fraction of the total load is free to slosh. In these cases, the relevant parameters are the percent of load being carried and the fraction of the load that is free to slosh.



## 1.6 Aims and Objectives

The basic aim of this research project is to study the lateral dynamics of heavy duty elliptical tankers carrying liquids loads. This is realized by using computer simulation packages to create models whose characteristics resemble that of a real vehicle. The objectives of this study can be broken into the following:

- Explore the capacity of *DynaFlexPro* and *DynaFlexPro/Tire* (multibody computer-aided engineering software packages) in the domain of modelization of vehicles. In order to achieve this, the most efficient method would be to gain in-depth knowledge of the software and its features by applying it in a certain domain of modeling. Following this idea the next objective is stated.
- Application of the software in the study of Rollover of Heavy Duty Articulated Tankers. Within this, the objectives can be further broken into the following:
  - As the vehicle is carrying liquid, sloshing effects will definitely intervene in the dynamics. So firstly a model is required to simulate the sloshing effects in elliptical tanks. For this phenomenon of sloshing, a model called trammel pendulum is chosen and to develop it model is the first task.
  - The second step will be to find a rational basis for selecting pendulum parameters to simulate sloshing in generic elliptical tankers with arbitrary level of fill.
  - Once the pendulum parameters have been set, the next step would be to create vehicle models of a tractor-trailer and to integrate the trammel pendulum. The vehicle model should be good enough to define the vehicle motion during turns and other basic tests.
  - Conduct parametric studies to assess the effect of variation of fill levels on the rollover stability of partially filled elliptical tankers.

# CHAPTER TWO

## MODELING OF THE FLUID IN ELLIPTICAL CONTAINERS BY TRAMMEL PENDULUM

### 2.1 Sloshing in Elliptical Tanks

The dynamic oscillation of liquid with a free surface has long been of interest in a variety of engineering fields. In particular, non-linear sloshing with large amplitudes and more complicated swirling motions are sometimes considered as the most important phenomena associated with the engineering design and assessment. These motions generate severe hydrodynamic loads that can be dangerous for structural integrity and stability of rockets, satellites, ships, trucks and even stationary petroleum containers. This problem of fluid sloshing in partially filled containers and its effect on vehicle stability concerned researchers for a long time. In heavy-duty tanker trucks the response of the vehicle to motions of the contained liquid may reduce the stability of the vehicle greatly. The oscillations, when allowed to continue, can create slosh forces that may have an adverse effect on the stability and structural integrity of the vehicle. In particular, if the liquid masses are excited at a frequency near that of a lower liquid mode, the amplitude of the liquid oscillations, and hence the resultant forces and moments, may be of such magnitude so as to induce instability to the vehicle. When liquid sloshing occurs in a spherical tank, for example, the maximum slosh forces approach a value equal to approximately one-fourth of the apparent weight of the contained liquid.

Sloshing in tanks can be caused by different manoeuvres of the vehicle due to the different steer inputs given. This section deals with the construction of an elliptical pendulum that will simulate the path of the center of gravity (cg) of fluid inside a partially filled elliptical tank. It describes the method used to demonstrate that the cg of the fluid mass inside an elliptical tank will follow an elliptical path proportional to the elliptical dimensions of the tank. It also includes the calculations of different angles of displacement, velocity, and acceleration for the elliptical trammel pendulum. Section 3.4 includes the calculations for different reactions at the support of the tank.

## 2.2 Mathematical Modeling of Sloshing in Elliptical Tanks

Previous literature has shown that the first lateral mode of sloshing in a container due to any lateral excitation is an anti-symmetric mode, and that it is the dominant mode. It was also determined that the angular movement of the straight line of the flat surface of the fluid (neglecting longitudinal sloshing) can present this anti-symmetric dominant mode [15]. Rakheja [9] and Salem [12] studied the location of the center of gravity for a given fluid in an elliptical tank assuming the surface motion above. Their study determined that the center of gravity of any fluid bulk translates along a concentric ellipse for a given fill level, lateral acceleration and sprung mass roll angle. Figure 2.2.1, shows the geometry of a partially filled elliptical tank and the path followed by the cg of the fluid volume at certain roll angle.

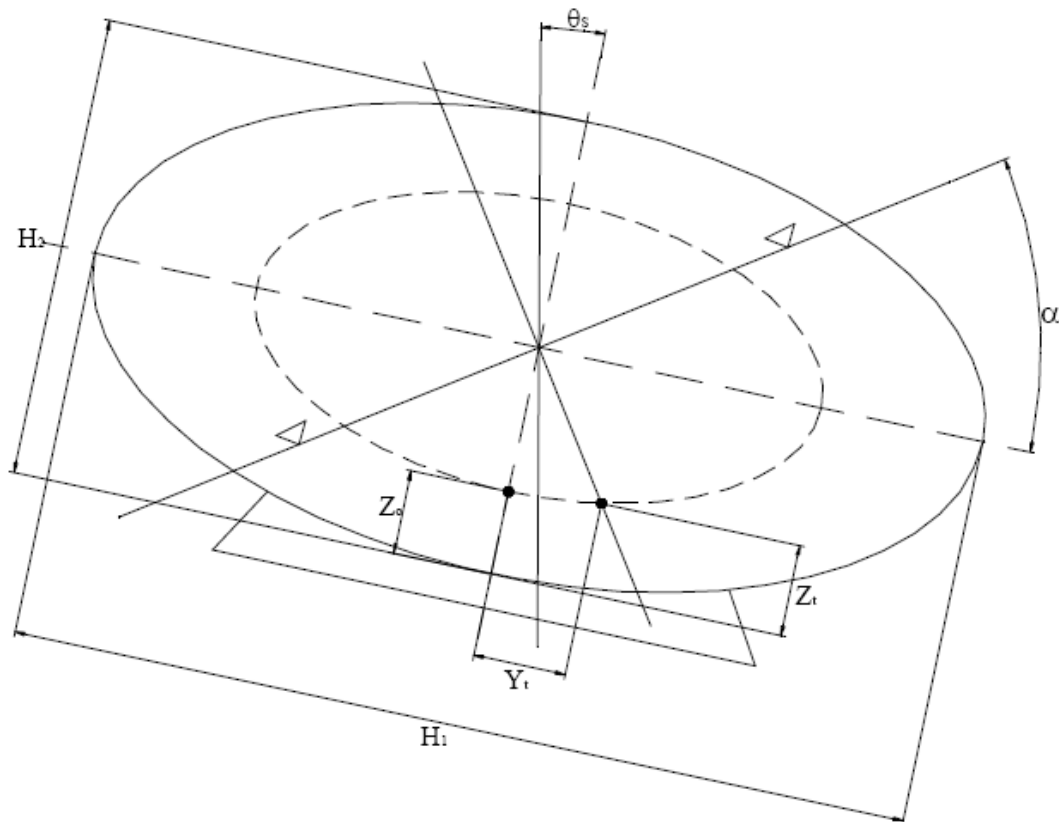


Figure 2.2.1: Steady State Motion of the Liquid Cargo under Vehicle Roll and Lateral Acceleration of an Elliptical Cross-section [9].

By assuming small angles ( $\tan(\theta) = \theta$ ), Rakheja expressed the gradient of the free flat surface of fluid ( $\alpha$ ) as a function of Tanker roll and angle ( $\theta_s$ ) and lateral acceleration ( $a_y$ )

$$\alpha = \frac{a_y + \theta_s}{1 - a_y \theta_s} \quad (2.2.1)$$

where ( $a_y$ ) is in g units and ( $\theta_s$ ) is in radians. The vertical and lateral coordinates of cg of an elliptical cross-section tank were derived from the geometry, and were expressed as:

$$Z_l = 0.5H_2(1 - \cos \alpha) + Z_0 \cos \alpha \quad (2.2.2)$$

By knowing the cg location of a partially filled elliptical tank, we automatically know the minor axis of the elliptical shape that the cg will follow. Figure 2.2.2 shows the path of the cg for an arbitrary partially filled elliptical tank. This path falls on a contour parallel to the tank wall such

$$\frac{\bar{a}_{cg}}{\bar{b}_{cg}} = \frac{\bar{a}}{\bar{b}} = \frac{a}{b} \quad (2.2.3)$$

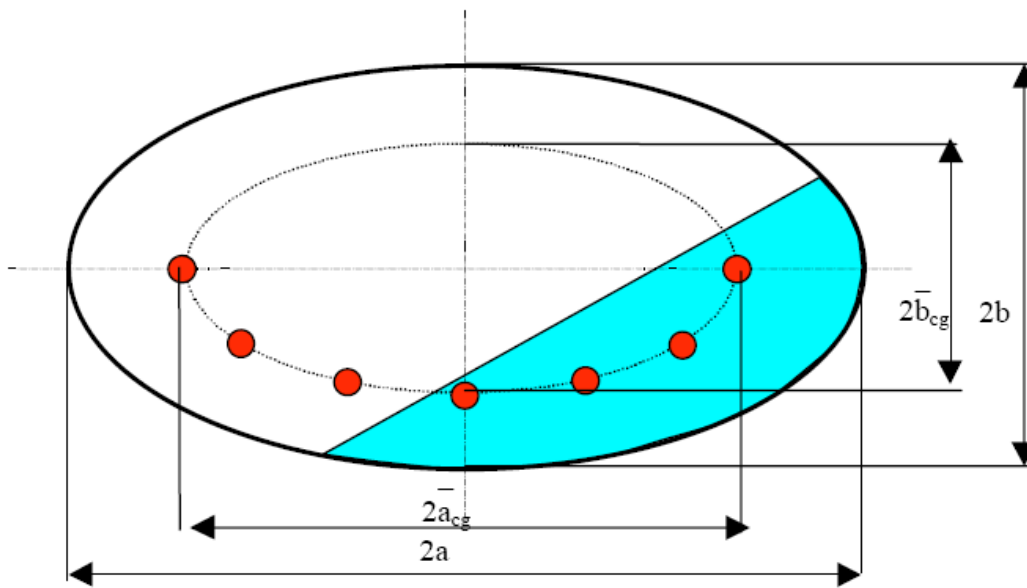


Figure 2.2.2: Locus of C.G. location for a given volume of fluid in an elliptical container

A trammel mechanism, which draws an elliptical path, was considered to simulate an elliptical pendulum (Figure 2.2.3).

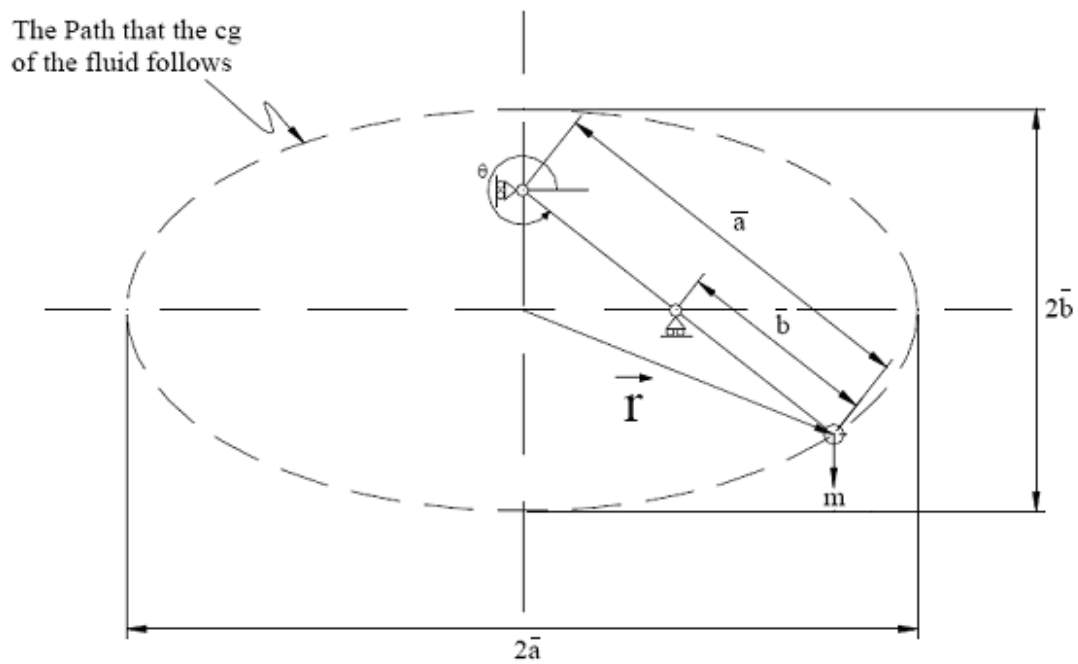


Figure 2.2.3: C.G. of fluid volume contour drawn by an elliptical trammel mechanism

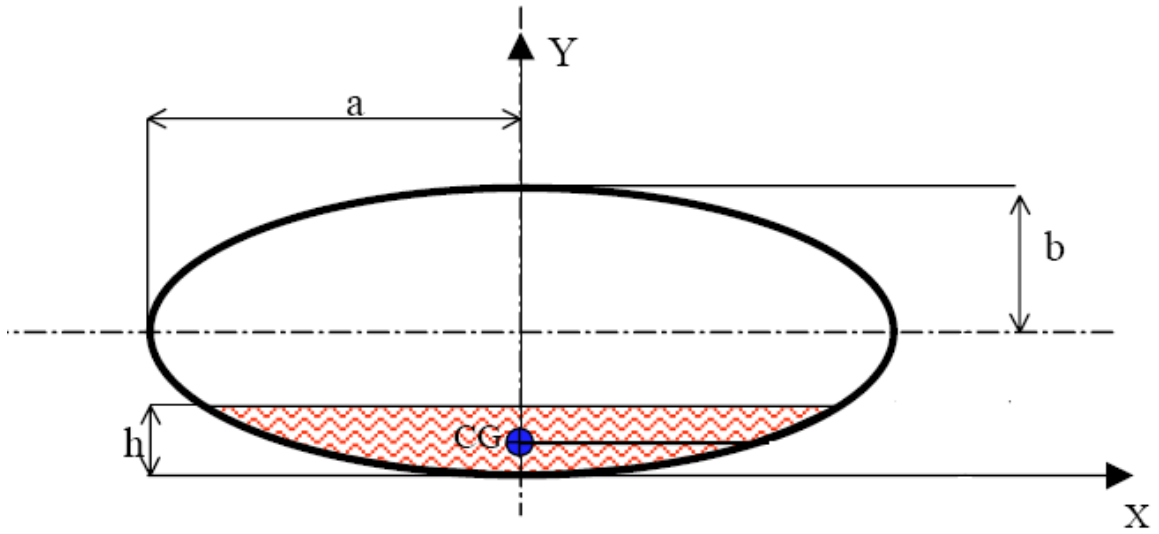


Figure 2.2.4: Diagram showing the fill level in an elliptical tanker.

The equation of motion for a trammel pendulum was given by (2.2.4)

$$\left( \bar{a}^2 \cos^2 \theta + \bar{b}^2 \sin^2 \theta \right) \ddot{\theta} + 0.5 \left( \bar{b}^2 - \bar{a}^2 \right) \dot{\theta}^2 \sin 2\theta + g \bar{b} \sin \theta + \bar{a} \cos \theta \ddot{x} = 0$$

For small angles this equation can be simplified as

$$\ddot{\theta} + \left( \frac{\bar{b}^2 - \bar{a}^2}{\bar{a}^2} \right) \dot{\theta}^2 \theta + \frac{g \bar{b}}{\bar{a}^2} \theta = 0$$

(2.2.5)

### 2.3 Trammel Pendulum Parameters

Salem compared the FE models for an elliptical tank with the same cross section area as the test tanker and  $a/b$  varying from 1 to 2. Using his FE model he determined the fundamental natural frequency of fluid slosh in a partially filled elliptical tank at different levels of fill. A small initial surface angle of 5 degrees was given to the fluid surface to maintain the linear assumption used to derive equation (2.2.5). Using this he compared his results to find the trammel pendulum parameters. By comparing the natural frequencies an approximate relation between  $\frac{\bar{b}}{b}$  and percentage fill was found to be:

$$\frac{\bar{b}}{b} = 1 + \left( 1.780896 + \frac{1.542048}{(a/b)} \right) \left( \frac{h}{2b} \right) + \left( 0.7726259 - \frac{1.304727}{(a/b)} \right) \left( \frac{h}{2b} \right)^2 \quad (2.2.6)$$

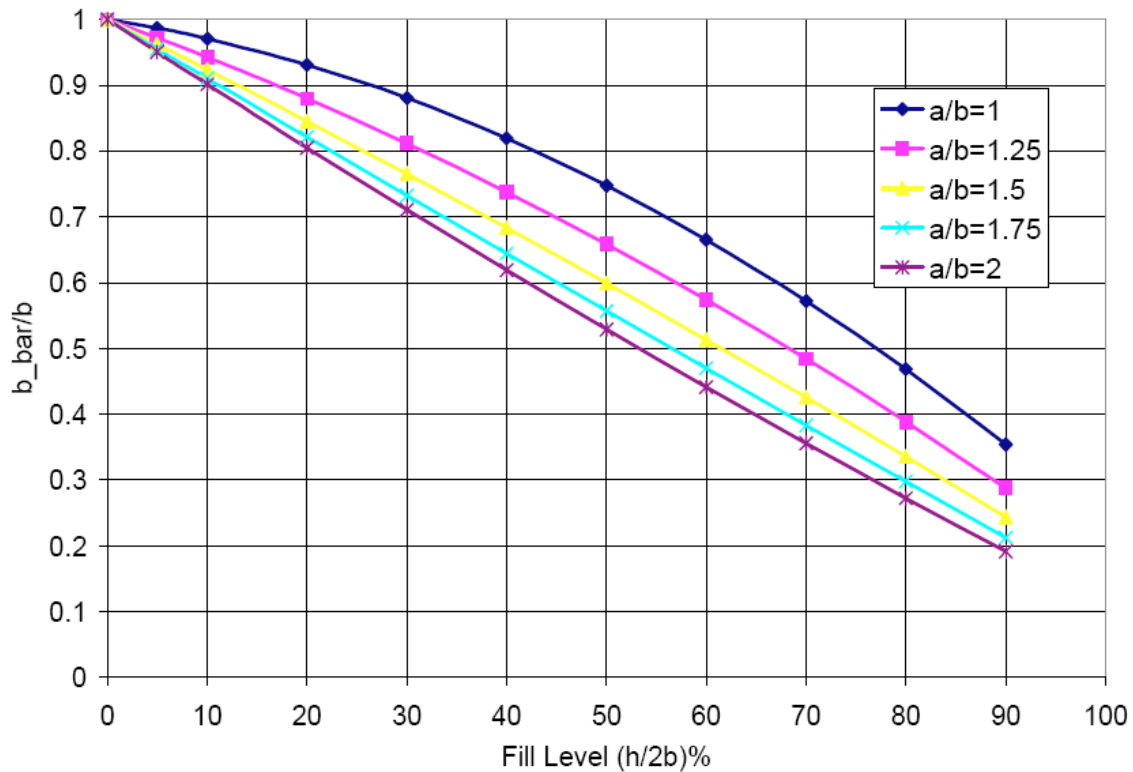


Figure 2.3.1:  $\bar{b}/b$  vs fill level for different values of  $a/b$

By comparing the lateral force equation the relation between mass of pendulum and percentage fill was found to be:

$$\frac{M_p}{M_t} = 1 + \left[ -0.863 + 1.237 \ln\left(\frac{a}{b}\right) \right] \left(\frac{h}{2b}\right) - \left[ 0.1226 + 1.2489 \ln\left(\frac{a}{b}\right) \right] \left(\frac{h}{2b}\right)^2 \quad (2.2.7)$$

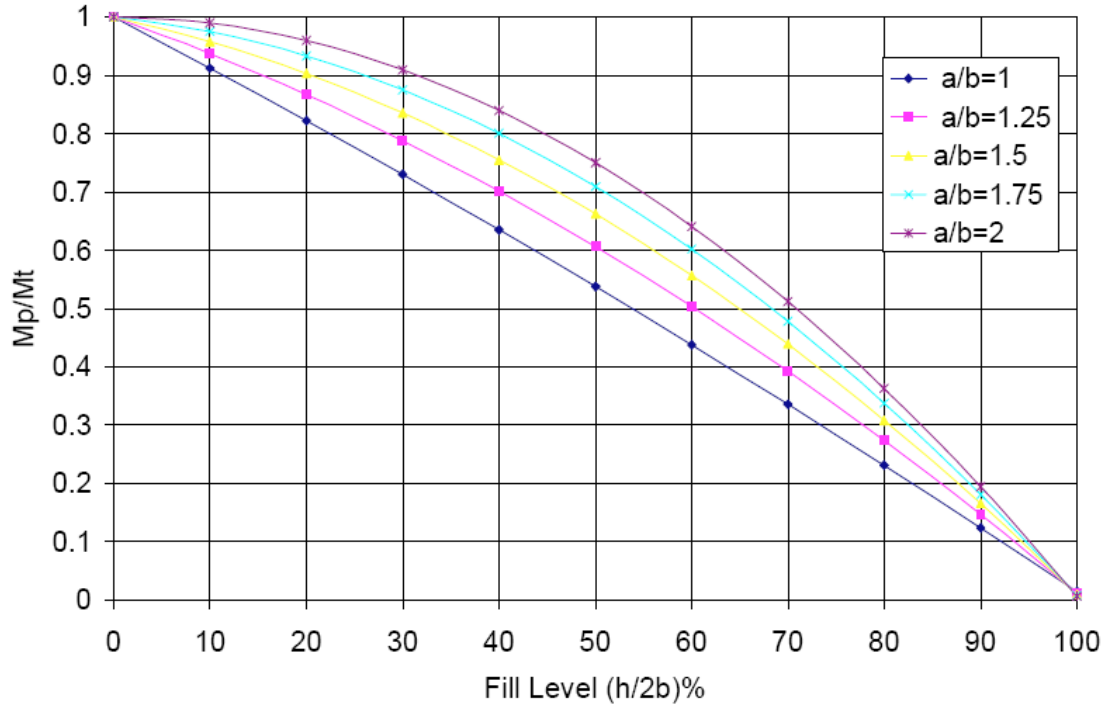


Figure 2.3.2:  $M_p/M_t$  vs fill level for different values of  $a/b$

The height of the fixed mass “ $h$ ” from the base point of the tank was found to be given by the relation:

$$\frac{h_o}{b} = \frac{Y_{CG} - \Phi b(1 - \Lambda)}{b(1 - \Phi)} \quad (2.2.8)$$

Where  $\bar{b}/b = \Lambda$  and  $M_p / M_t = \Phi$ .



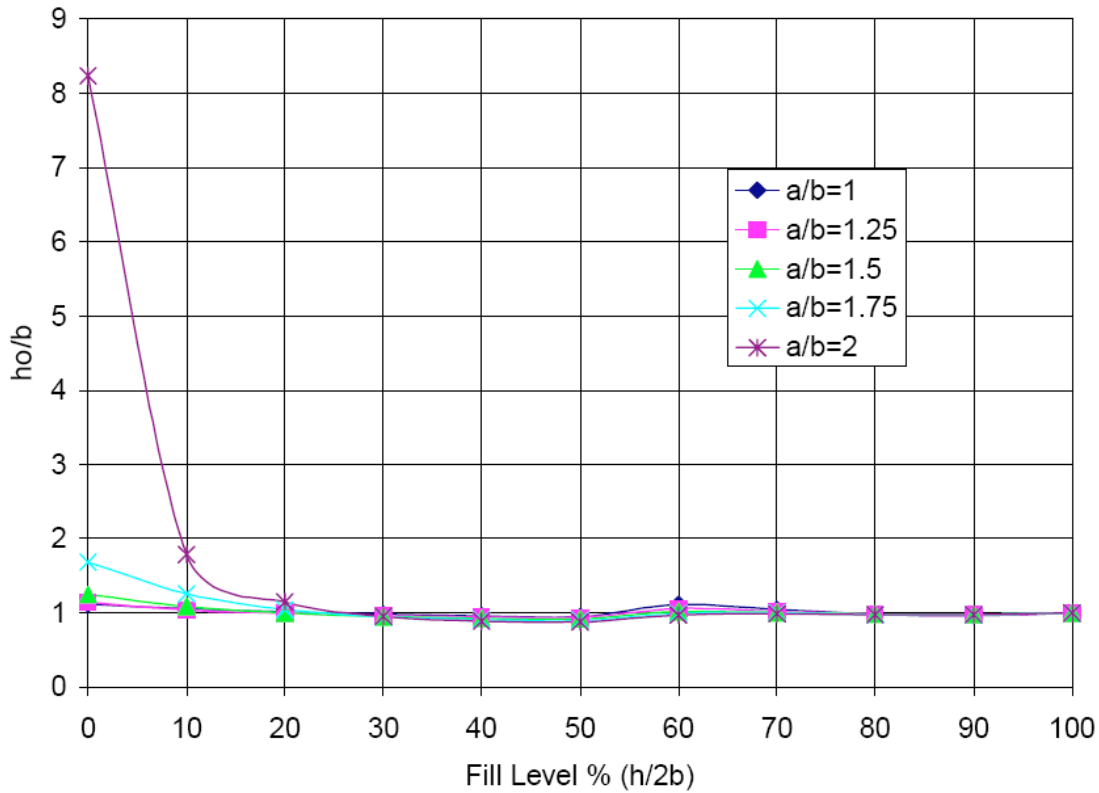


Figure 2.3.3:  $h_o/b$  vs fill level for different values of  $a/b$

## 2.4 *DynaFlexPro* Trammel Pendulum Model

### Introduction to *DynaFlexPro*

For the modeling environment, we chose the *DynaFlexPro* which is a multibody computer-aided engineering software package released by MotionPro Inc. and distributed by MapleSoft, Inc., of Waterloo, Ontario.

*DynaFlexPro* is a collection of Maple routines that will automatically generate the symbolic equations of motion for an inter-connected system of rigid bodies and flexible beams, given only a description of the system as input. In other words, *DynaFlexPro* (DFP) is a symbolic package for multibody dynamics.

By eliminating the tedious and error-prone task of deriving equations by hand, DFP allows a user to focus on the analysis and design of a given physical system. To date, *DynaFlexPro* has been used to model robots (serial and parallel), road and rail vehicles, many different mechanisms and machines, and biomechanical systems.

*DynaFlexPro* supports a library of modeling components, including rigid bodies, flexible beams, forces, torques, springs, dampers, and a variety of joints (revolute, spherical, universal, etc.). Unlike other multibody computer programs, *DynaFlexPro* allows the user to select the coordinates appearing in the final equations of motion.

These symbolic equations can be visually examined, exchanged with colleagues, numerically integrated within Maple, or exported as optimized simulation code (C, FORTRAN, Matlab, etc) to another package.

*DynaFlexPro* is a system that is constantly under development. New features, such as electrical components and transducers for modeling electrical networks and mechatronic systems, tire models for vehicle dynamics, and hydraulic models are currently being tested and will be made available in the future.

### Trammel Pendulum Model

The trammel pendulum was modeled according to the figure shown below:

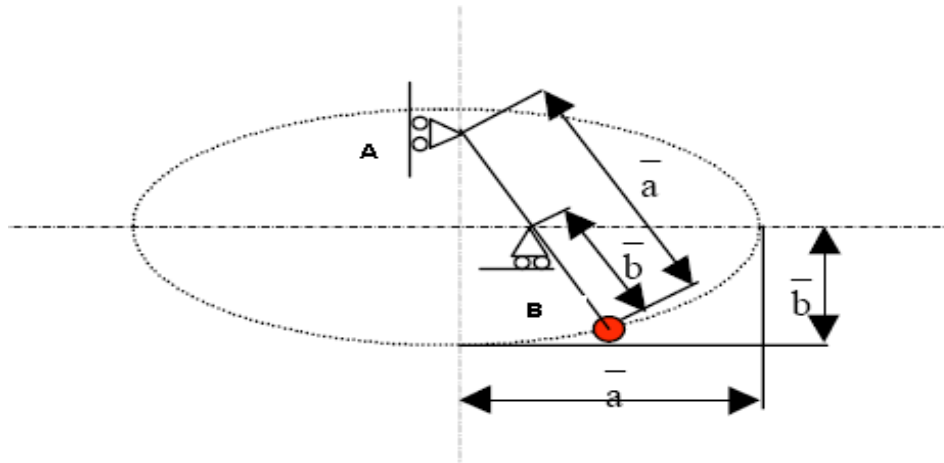


Figure 2.4.1: Trammel Pendulum

The joints between sliders A and B and ground were modeled as prismatic joints with their axis of translation in horizontal and vertical direction. The sliders A and B are massless bodies having a revolute joint with the pendulum. The values  $\bar{a}$  and  $\bar{b}$  which are functions of fill level can be found from the appendix [5]. Shown below is the model for the trammel pendulum. The Maple code for the generation of the model equations and diagrams can be found in the appendix [1].

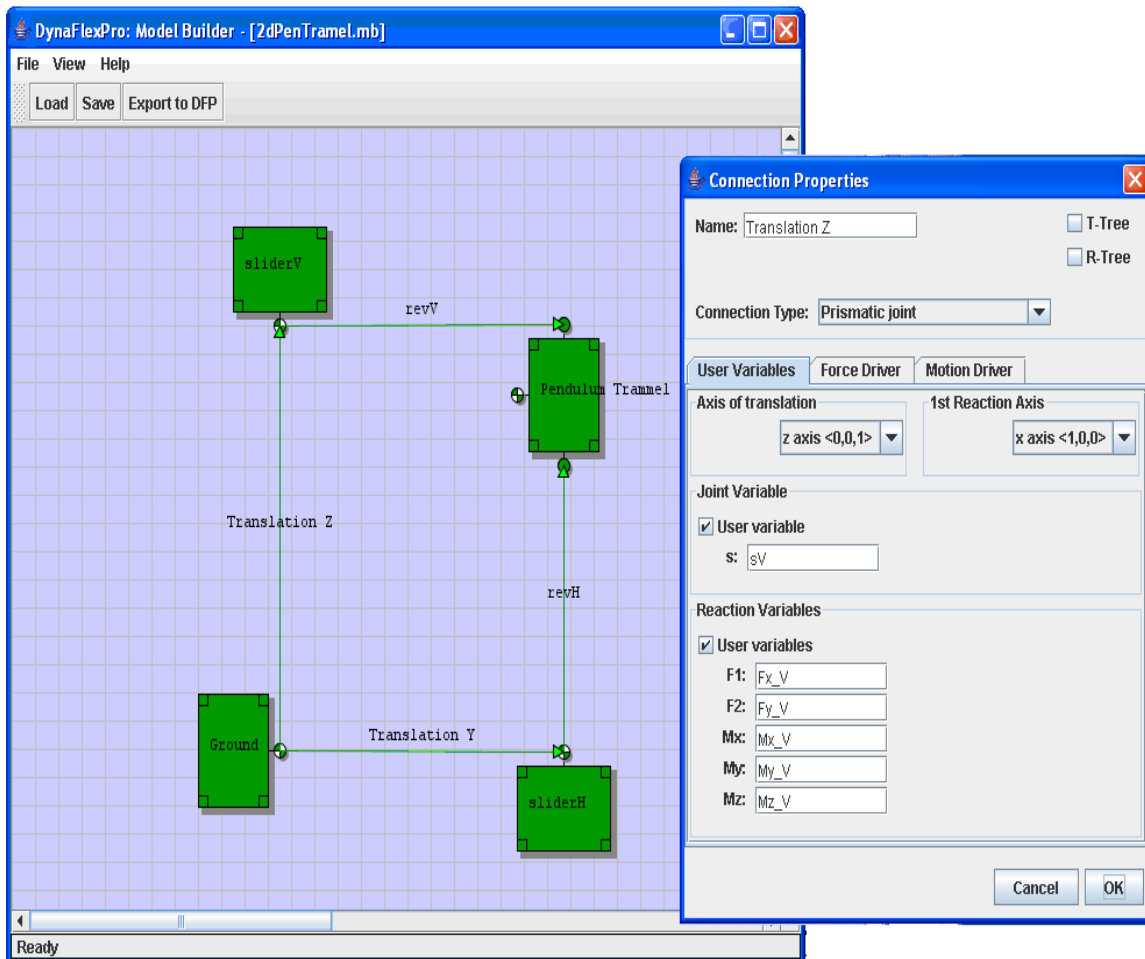


Figure 2.4.2: DynaFlexPro model of Trammel Pendulum.

## 2.5 Simulation and Results

The pendulum was given different initial angles of 5, 30, 60, 90 and 150 degrees for the value of aspect ratio ( $a/b=1.2/0.6905$ ) and the natural frequencies were found out. The plots below show the position and velocity of angles at different initial angles.

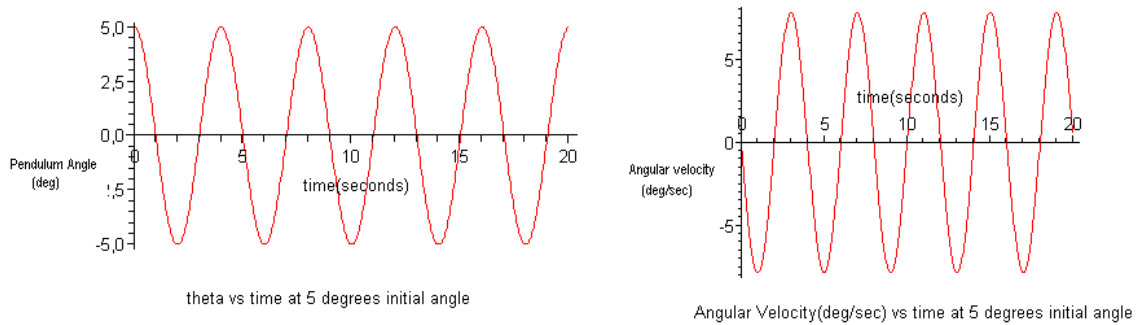


Figure 2.5.1: Position and Velocity of Pendulum angle at 5 deg initial angle

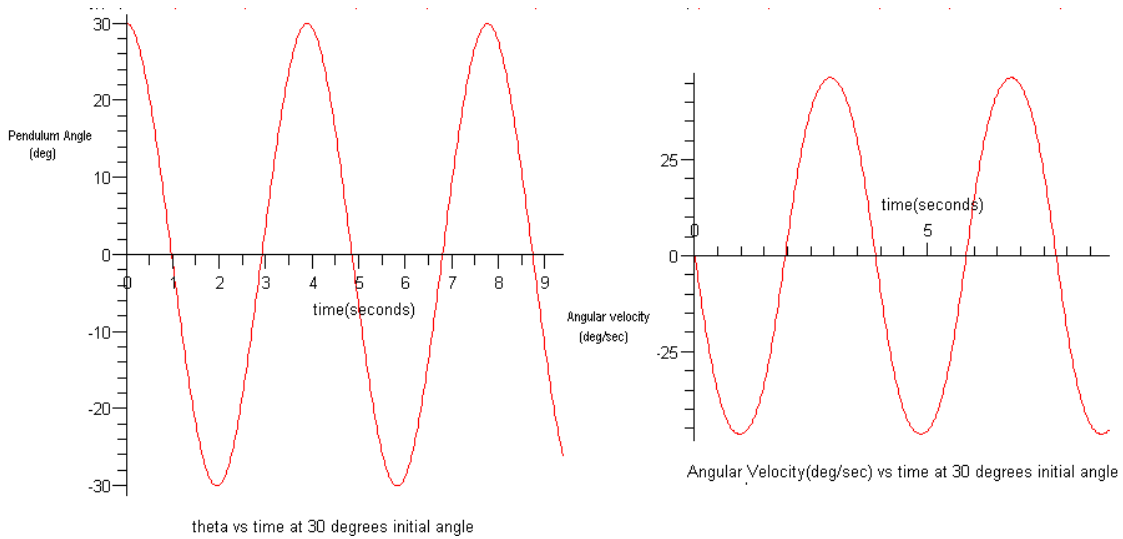


Figure 2.5.2: Position and Velocity of Pendulum angle at 30 deg initial angle

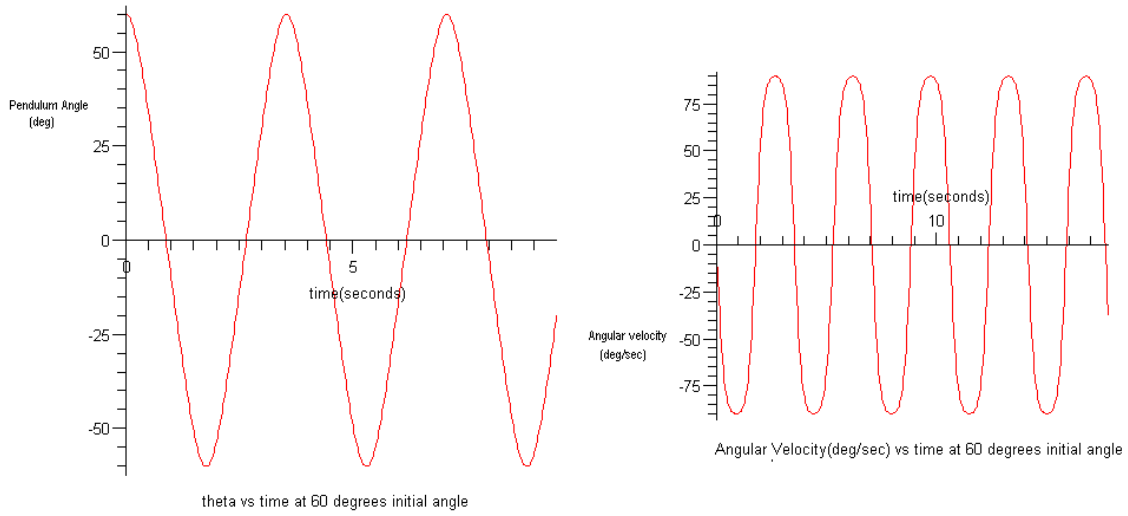


Figure 2.5.3: Position and Velocity of Pendulum angle at 60 deg initial angle

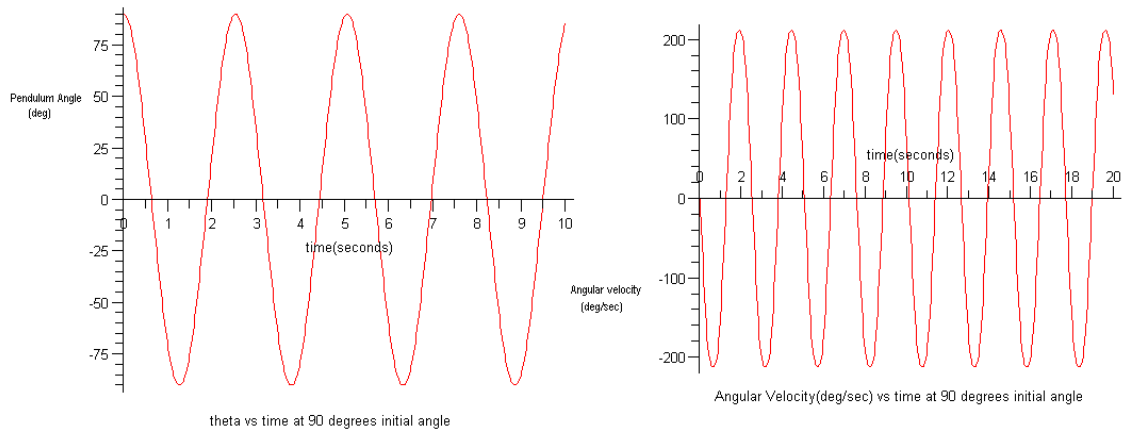


Figure 2.5.4: Position and Velocity of Pendulum angle at 90 deg initial angle

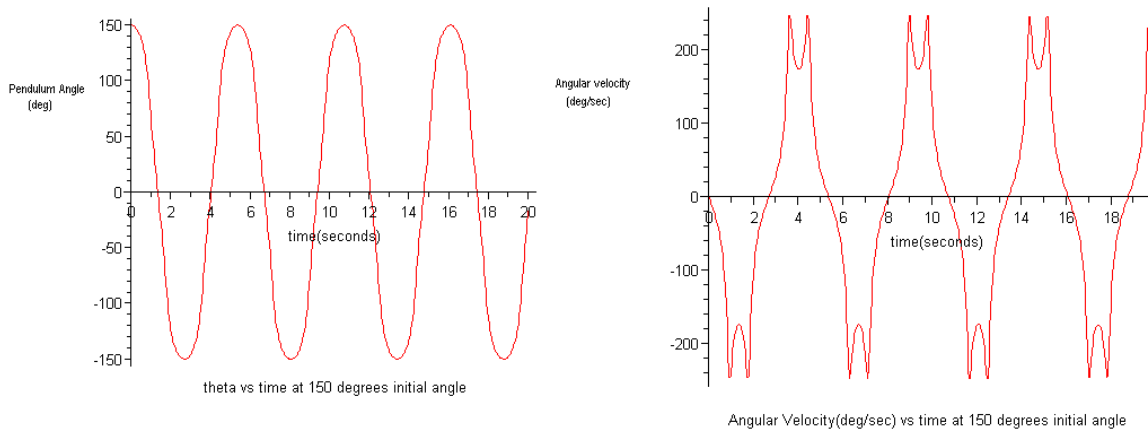


Figure 2.5.5: Position and Velocity of Pendulum angle at 150 deg initial angle

The plot below shows the natural frequency as a function of fill level for a 5 degree initial angle. The parameters of the tank chosen are  $a= 1.2$  and  $b=0.6095$ . which are the same as that of the tanker shell. Also the mass of pendulum and other parameters at different fill levels have been taken from the actual model and these parameters have been used further in our simulations. These natural frequencies found out using Trammel Pendulum model have a very similar values with the natural frequencies found out by Salem using Finite Element Models. The plots below shows the natural frequencies found by the trammel pendulum followed by the plot of natural frequencies found by Salem using his FE model for an initial angle of 5 degrees.

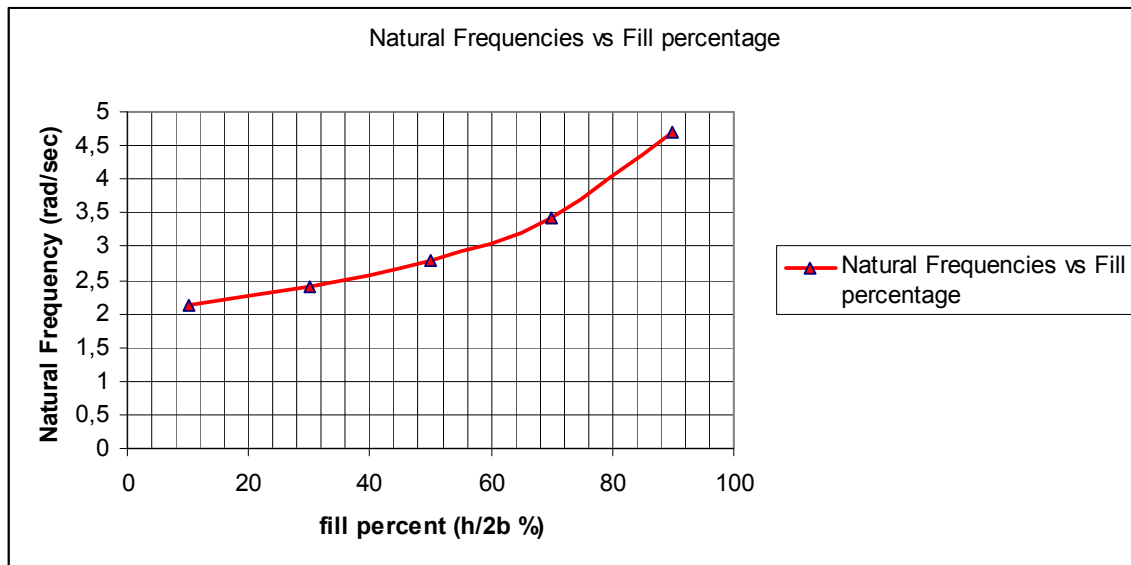


Figure 2.5.6: Natural Frequency vs fill level for 5 degree initial angle

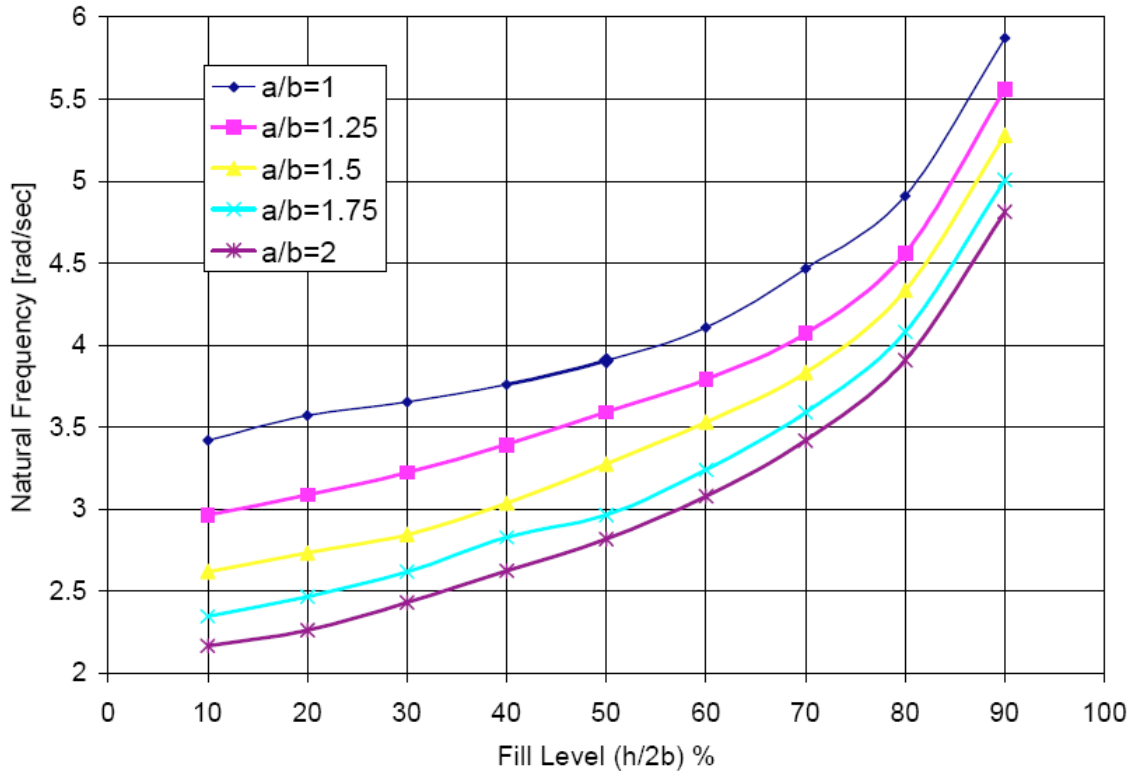


Figure 2.5.7: Natural frequency vs. fill level for a fluid volume in an elliptical tank with different values of  $a/b$  at initial fluid surface angle =5 degrees obtained using FEM by Salem.

# CHAPTER THREE

## VEHICLE MODELS AND SIMULATION

A good dynamic model is an essential tool for assessing the performance characteristics of a vehicle. The difficulty in creating the model comes from determining the appropriate level of detail that will accurately represent the dynamics of interest. Too much detail and analysis becomes unnecessarily complicated. With too little detail, the model fails to sufficiently resemble the real system.

As an example, the commonly used four-degree of freedom truck model—the degrees being lateral position, longitudinal position, yaw angle, and trailer articulation angle—while useful for many types of analyses, lacks information about roll angle. During normal driving, roll dynamics can be safely neglected for cars, but for a truck, especially if it is heavily loaded, even a mild turning manoeuver may place it in danger of rolling over completely. In addition, due to the particular kinematics of truck suspensions, body roll produces an additional steering effect known as roll steer. By using a somewhat more complicated representation than the four-degree of freedom model—one that includes suspension kinematics—we can capture dynamics critical to safety performance that would otherwise be lost.

### 3.1 Introduction to *DynaFlexPro/Tire*

For the modeling environment, we chose the *DynaFlexPro and DynaFlexPro/Tire* which is a computer software package distributed by MapleSoft.

*DynaFlexPro* is widely used in the mechanical industry for simulating complex mechanical systems dynamics. *DynaFlexPro/Tire* is an optional module to *DynaFlexPro* for modeling and simulating dynamics of complex mechanical multibody systems. The module lets engineers use pneumatic tire models in simulating vehicle systems. The software derives kinematic quantities, such as slip angle, longitudinal slip, and camber angle, as optimized computational sequences. These are used by tire models to find tire forces and moments. Optional features let users control how tire slip and rolling radius



are calculated and include tire transients through differential equations involving relaxation lengths. The program works with *DynaFlexPro/Model-Builder*, a GUI for creating models using block diagrams and drop-down menus.

The *DynaFlexPro* Model designed targeted on a certain specific type heavy duty tractor trailer vehicle. The specific vehicle chosen was full-scale army tanker truck (M916A1/Entyre 60 PRS 6000-Gallon Water Tanker) shown in Figure 3.1.1.



Figure 3.1.1: Tanker used for modeling

The simple picture of the truck is not sufficient for the modeling and some in-depth parameters and design features are needed as rolling stiffness, position of suspensions etc. Since a complete parametric set was not available most of the data was approximated from the literature available. The following figures and tables shows the parametric set of values used.

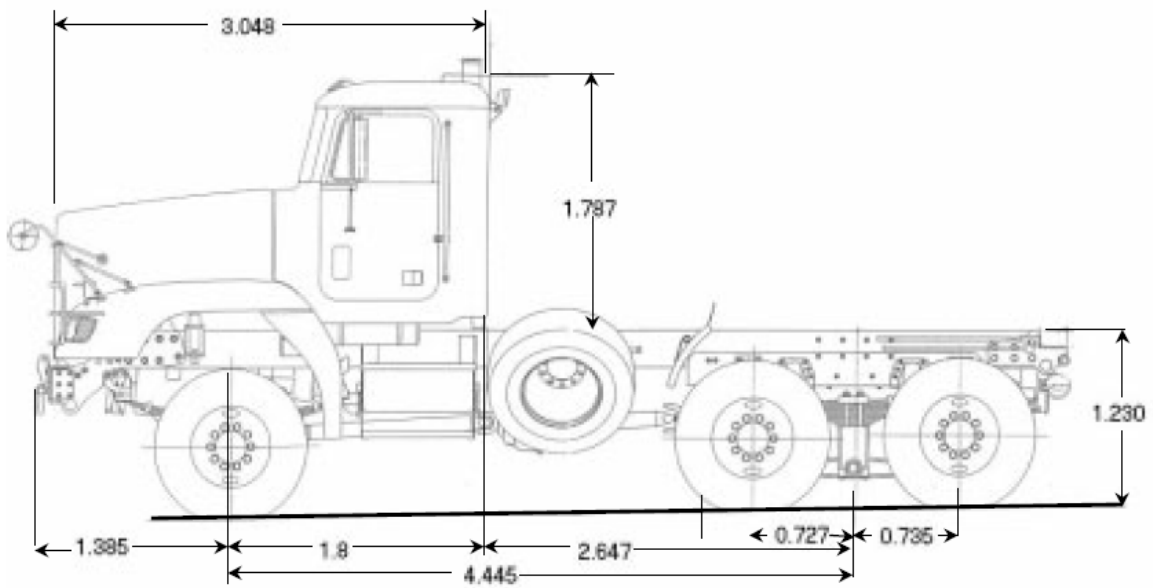


Figure 3.1.2: Main dimensions of the Tractor.

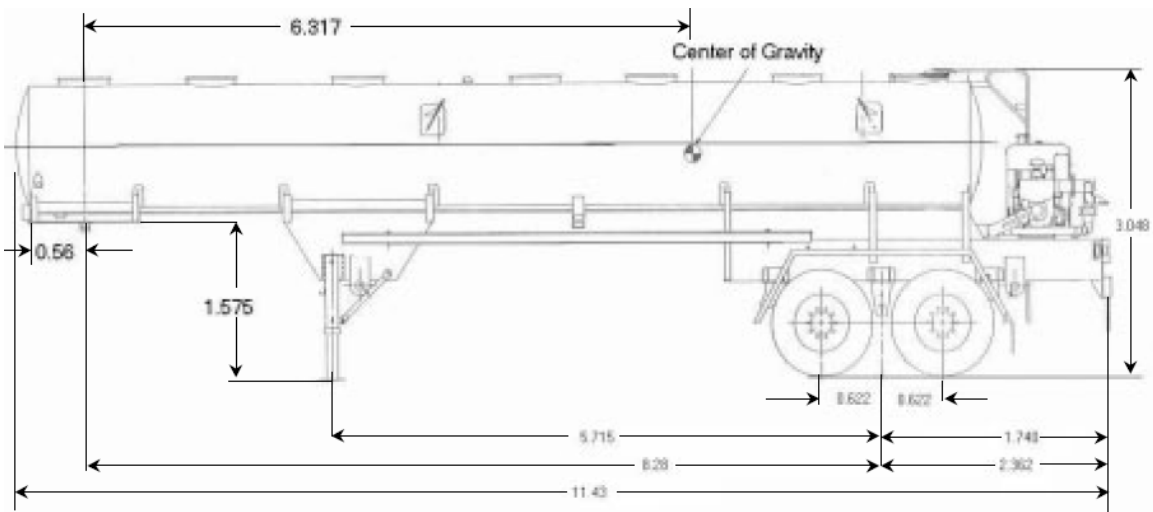


Figure 3.1.3: Main dimensions of the Trailer.

Other parameters:

Table 3.1.1: Parameters of vehicle.

<b>Parameter</b>	<b>Value</b>
<b><u>Masses</u></b>	
Tractor Only	12,000 kg
Trailer Only – Empty	63,00 kg
Trailer Only – Full	28,300 kg
Axles	145 kg each.
Wheels	37.2 kg each.
Tires	50.3 kg each.
Hub & drum	39.7 * 2. each.
<b><u>Spring Stiffness</u></b>	
Tractor Front Suspension (Vertical)	337805 N/m
Tractor Front Suspension (Rotational)	150000 Nm/rad
Tractor Rear Suspension (Vertical)	2017348 N/m
Tractor Rear Suspension (Rotational)	400000 Nm/rad
Trailer Suspension (Vertical)	1800000 N/m
Trailer Suspension (Rotational)	850000 Nm/rad
Tire Stiffness (Vertical)	870000 N/m
<b><u>Spring Dampings</u></b>	
Tractor Front Suspension (Vertical)	150000 Ns/m
Tractor Front Suspension (Rotational)	15000 Nms/rad
Tractor Rear Suspension (Vertical)	310000 Ns/m
Tractor Rear Suspension (Rotational)	31000 Nms/rad
Trailer Suspension (Vertical)	350000 Ns/m
Trailer Suspension (Rotational)	35000 Nms/rad

Tire Stiffness (Vertical)	10000 Ns/m
<b><u>Heights of Roll Centers</u></b>	<b>above ground level</b>
Tractor Steer Axle	0.473 meters
Tractor Drive Axle	0.657 meters
Trailer Axle	0.736 meters
Tire radius (actual)	0.515 meters
Tire radius (rolling)	0.5 meters

A number of vehicle models were created in *DynaFlexPro* to study the effects of sloshing on the dynamics of the vehicle. The Trammel Pendulum Model which was built to simulate the forces of sloshing was mounted on each of the vehicle. Firstly, very simple models were created starting from 2 dimensional roll models and slowly the complexity was increased until a full 3 dimensional working vehicle model was achieved.

Two basic tests were conducted on the all the vehicle models to study its rollover dynamics. Firstly, the Clothoid test or entering a curve test and then the Lane Change Manoeuvre.

Entering a curve can be described as a continuous transition from a straight line with curvature  $k=0$  to a circle with a curvature  $k=constant$ . During this transition the lateral acceleration seems have a linear profile starting from zero to a fixed value. This curve removes the discontinuity of the acceleration while the vehicle makes a transition from a straight line to a circle. It is very common to find the design of highways as a clothoid curve. A clothoid curve can be seen below:

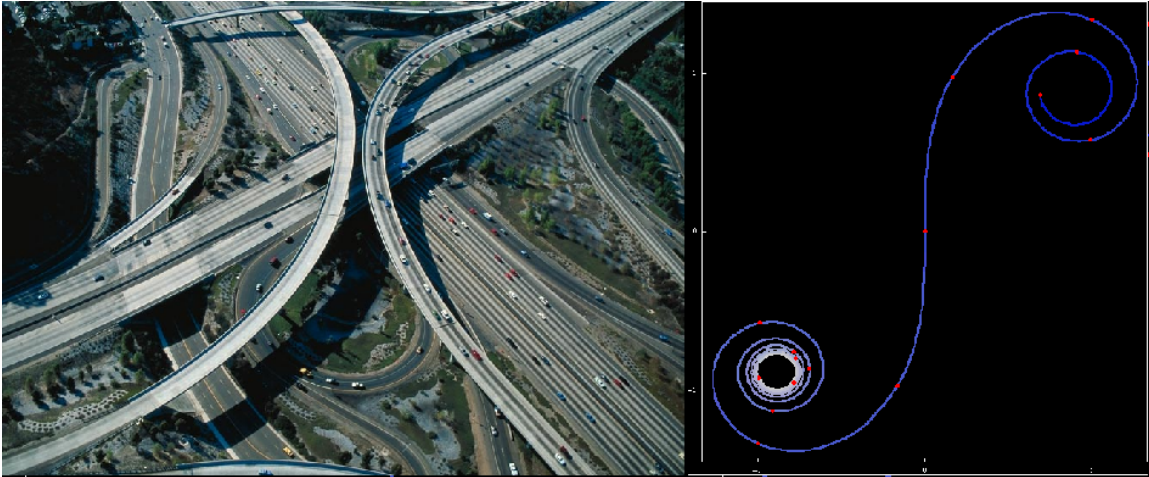


Figure 3.1.4: Design of highways by clothoid curve (left) and a simple clothoid curve (right).

The second test was the Lane Change Manoeuvre or obstacle avoidance test. The figure below gives a better understanding of the test. This test is to determine the reactivity of the vehicle. As the 2-D vehicle did not have a driver model, sinusoidal steer inputs were given and the maximum lateral accelerations at which the vehicle overturned was found out.

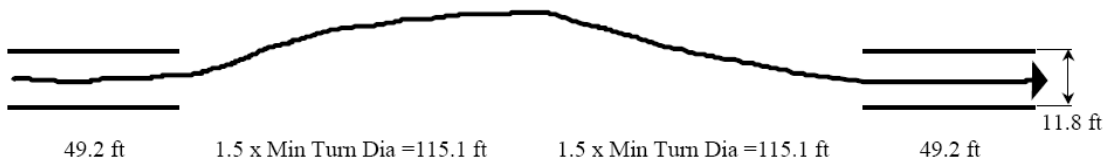


Figure 3.3: Path of the test vehicle during the TOP Lane Change Test

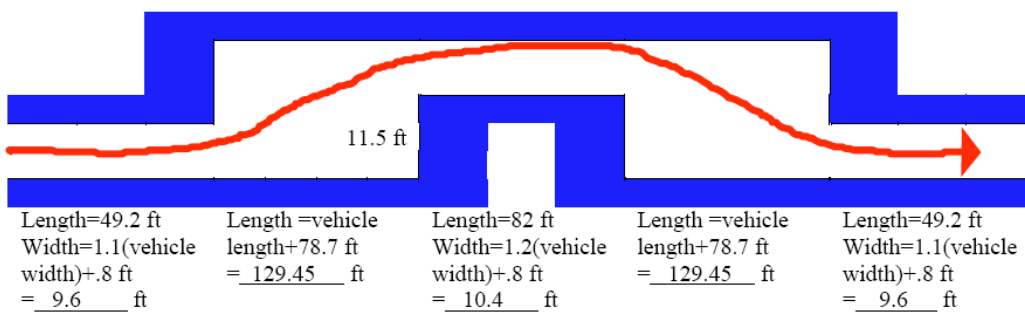


Figure 3.1.5: Lane Change Manoeuvre - NATO (AVTP 03-160W)

### 3.2 2-D Models

The effect of sloshing on the dynamics of the vehicle is mainly on its rollover. As we were studying the dynamics of Heavy articulated commercial vehicles, which are mostly prone to rollover, considering only a roll plane model was an appropriate initial step.

Among the Tractor and Trailer, the tractor is considerably more stably compared to a trailer. During a manoeuvre the trailer loses stability faster than a tractor. In terms of lateral acceleration the tractor is able to withstand higher values of lateral acceleration where as a trailer rolls over at 0.3g. Taking these facts under consideration we can safely remove the tractor and consider only the 2-D roll plane of the Trailer.

A simple roll plane model of the trailer unit was necessary in order to do an initial study of the vehicle response and behavior. The model is shown in Figure 3.2.1. It has three degrees of freedom, namely the rotation about the cistern roll axis, rotation of axle about the suspension c.g. and the trammel pendulum angle. Both the trailer axles are condensed into one axle, whose properties are equivalent to the sum of the three trailer axles. The Cistern mass rolls about the roll centre located 0.736 m above the ground, which is an average location for a tandem two axle type.

The 2-D roll model of the Trailer can be better understood from the figure below.

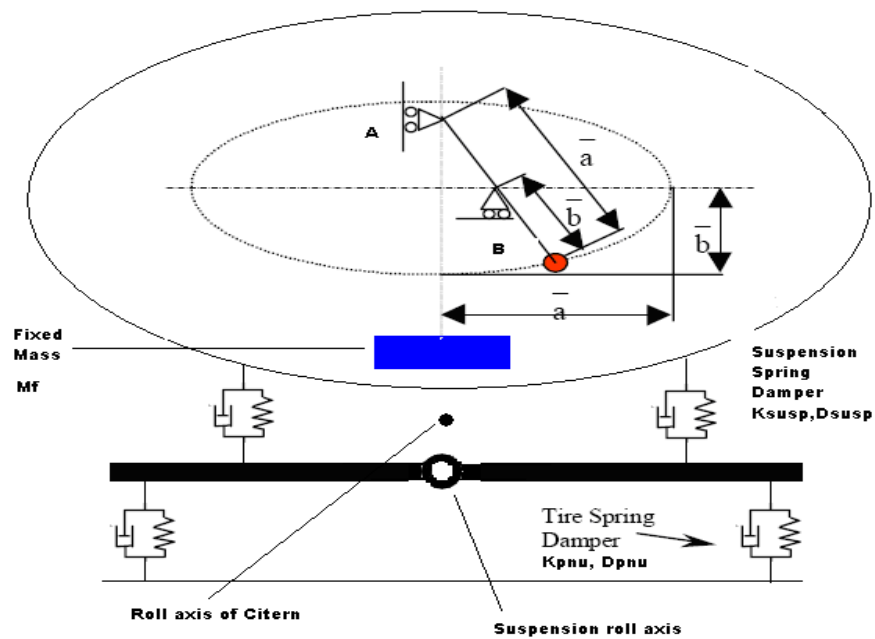


Figure 3.2.1: 2-D Roll model of the Tanker

The DynaFlexPro model for this system can be seen below:

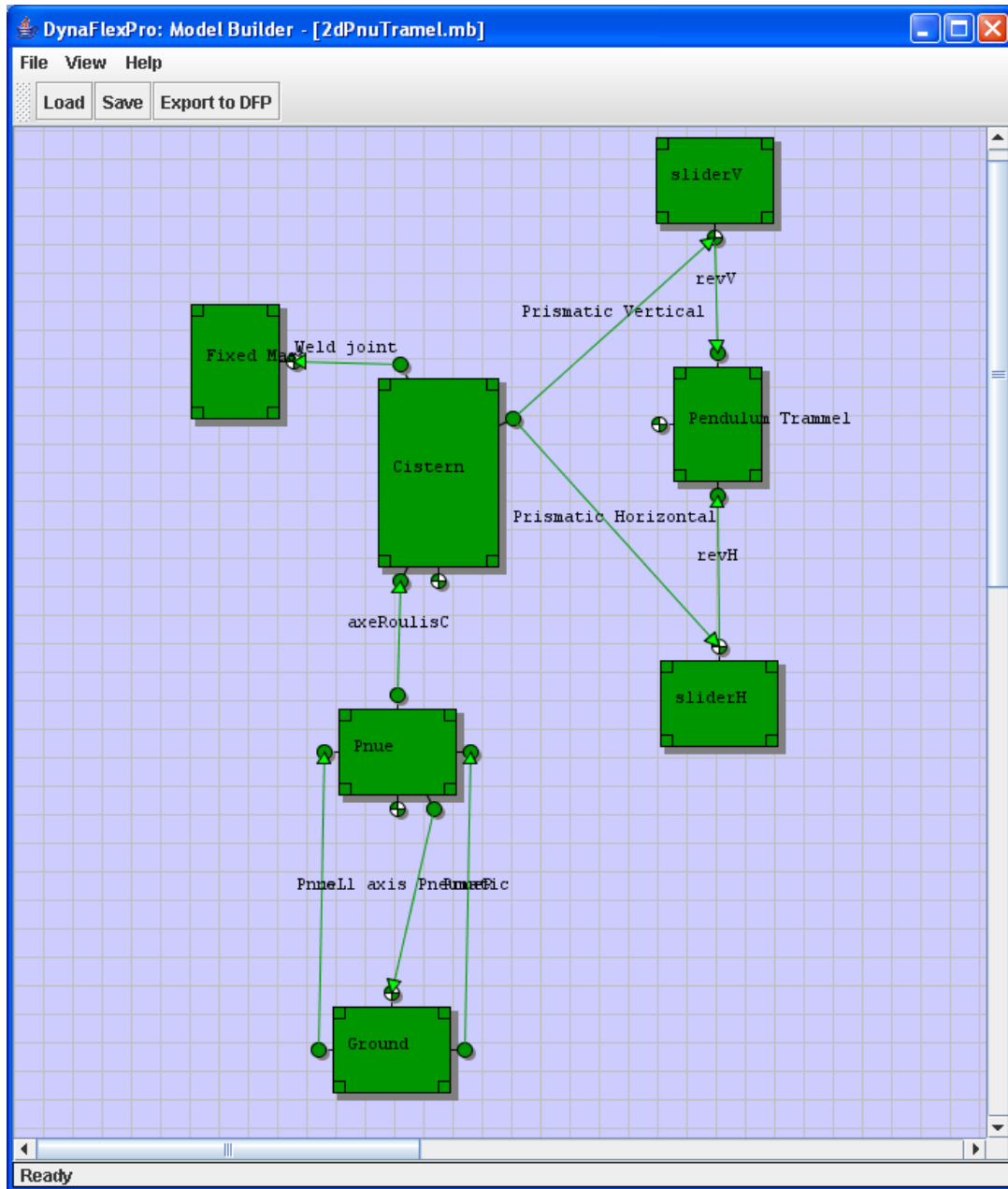


Figure 3.2.2: DynaFlexPro model for 2-D model.

This model was subjected to two different kinds of manoeuvre tests, the clothoid and the Lane Change Manoeuvre. As this is a 2-D model exact tests could not be performed so the tests were simulated by giving lateral accelerations of the same profile which it undergoes during the tests. Rollover was considered when the center of the left wheel had a height of  $0.515$  above ground level. The initial distance was kept as  $0.5$  meters which is the rolling radius of the tire and when the distance was more than  $0.515$  meters *i.e.* the actual radius, Lift Off was considered.

While entering a clothoid curve the lateral accelerations can be seen to be a ramp function which starts from zero. So the model was given a linear lateral acceleration for some time and then kept constant.

$$LateralAcceleration := \begin{cases} 4a t & t \leq 10 \\ 10a & t > 10 \end{cases}$$

The values of “ $a$ ” were chosen according to each test performed.

Sample plot of Lateral acceleration can be seen below.

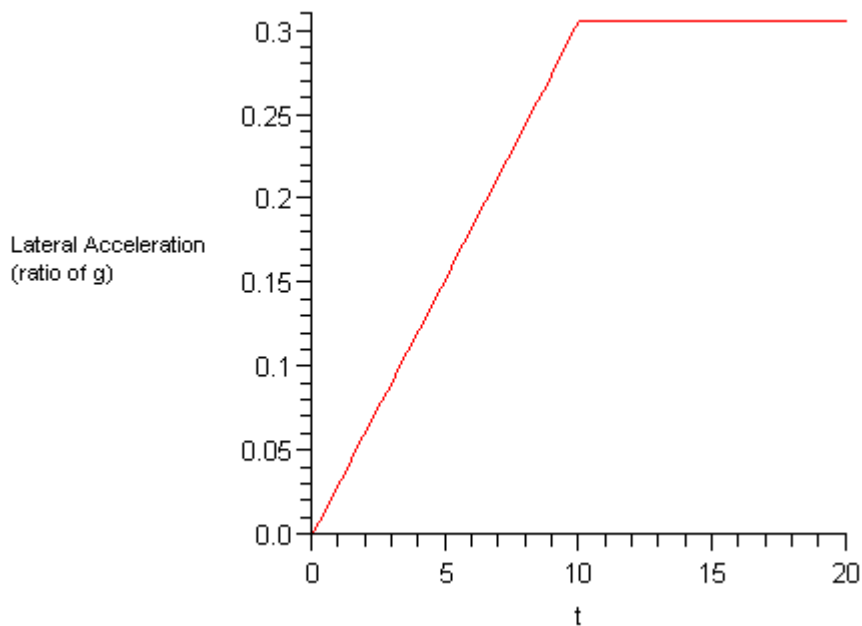


Figure 3.2.3: Lateral Acceleration vs time for a Clothoid test



During a Lane Change Manoeuvre the lateral acceleration was found to have a sinusoidal profile. Thus the function F was given as:

$$\text{LateralAcceleration} = A * \sin(2\pi * t/3)$$

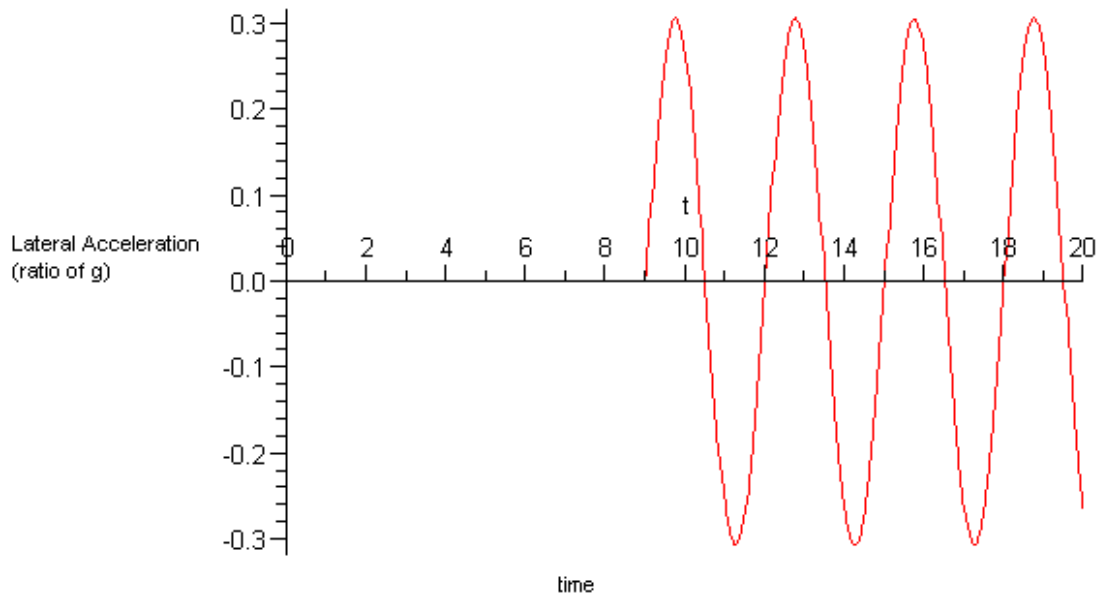


Figure 3.2.4: Lateral Acceleration vs time for a Lane Change Manoeuvre.

The results found from the tests simulated on the can be shown as below.

### **Clothoid Test:**

Tests were conducted for different levels of fills. These tests gave a very conservative approximation of the vehicle model. As expected the effect of sloshing did play a major role in the rollover threshold. Highest accelerations of 0.85g were reached when then fill level were zero. This threshold varied a lot depending on the fill level to a minimum of 0.25g for a fill level of 100%. For a fill level of 50 % the following plots were recorded.

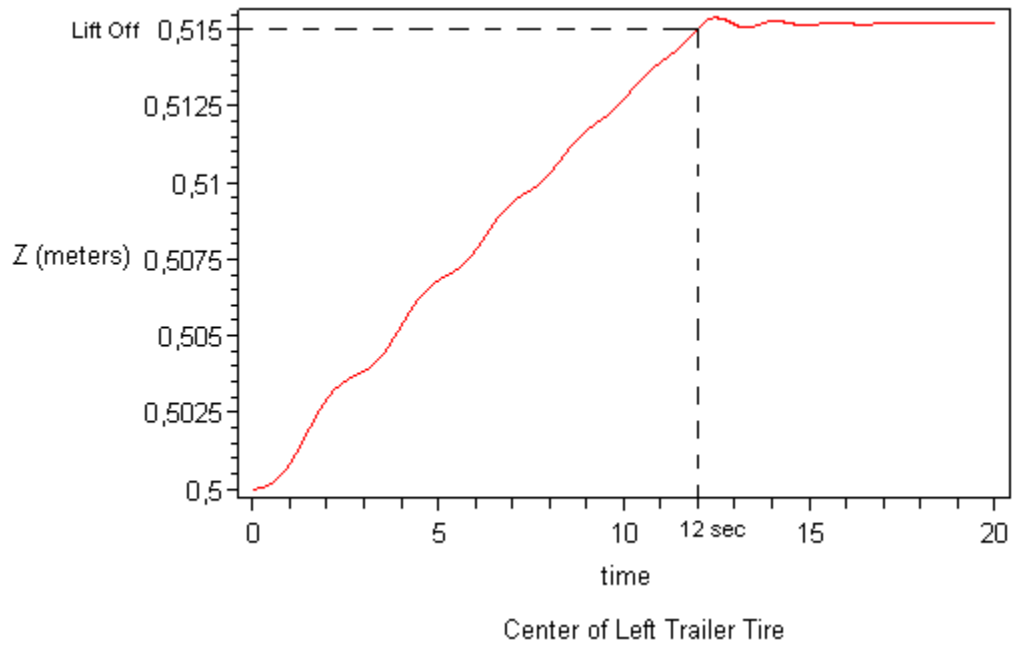


Figure 3.2.5: Vertical displacement of center of left tire with respect to ground for a 50% fill level during a Clothoid Test.

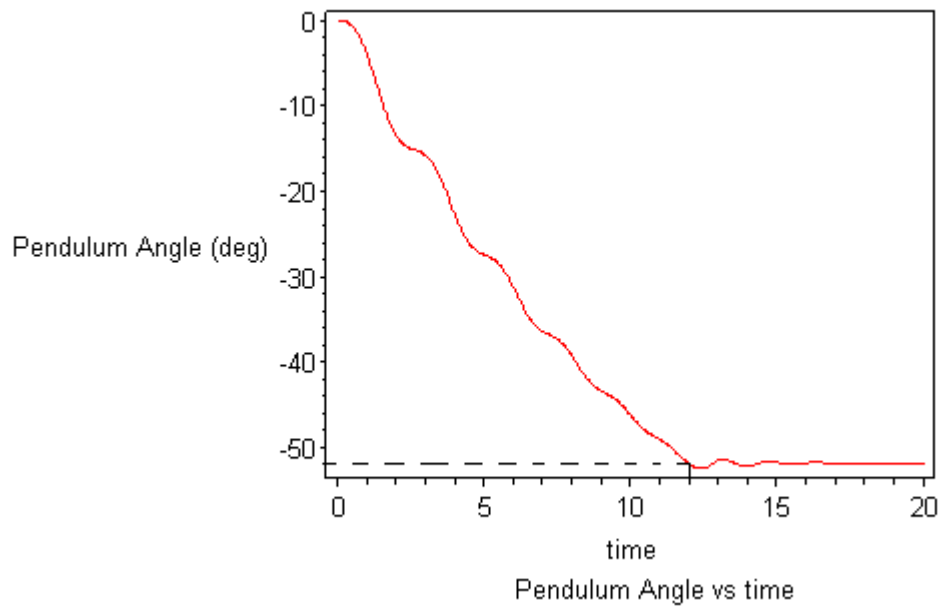


Figure 3.2.6: Pendulum angle vs. time for a 50 % fill level during a Clothoid Test.

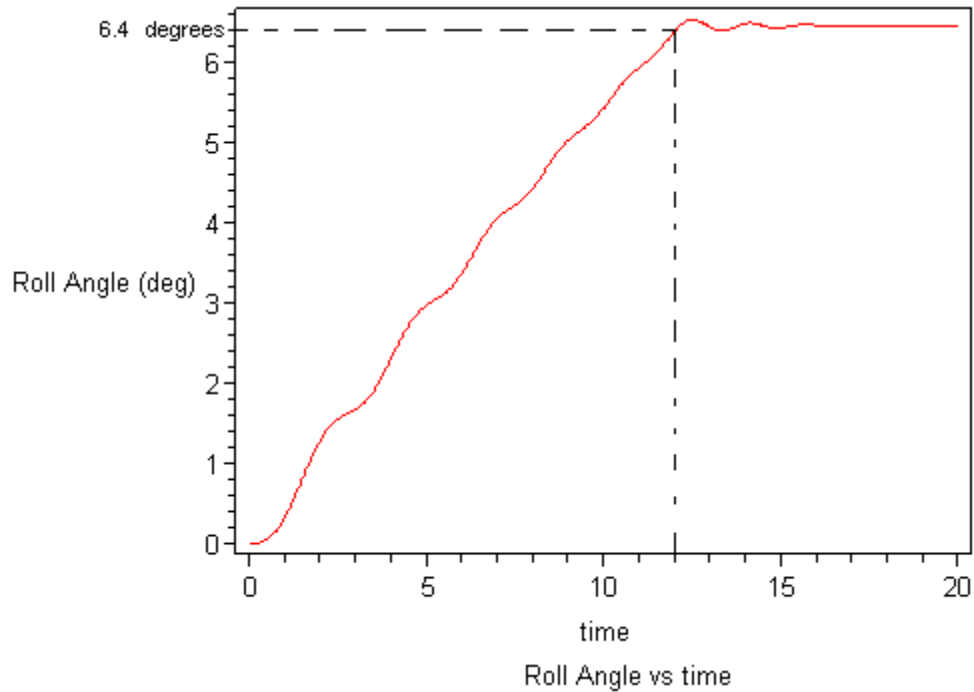


Figure 3.2.7: Change of roll angle vs. time for a 50% fill level during clothoid test.

The following plot shows the variation of the lateral acceleration with change in fill level. A sudden dip in values around 50% fill level is observed which continues till the 70 % mark showing the effect of sloshing on the vehicle's lateral stability.

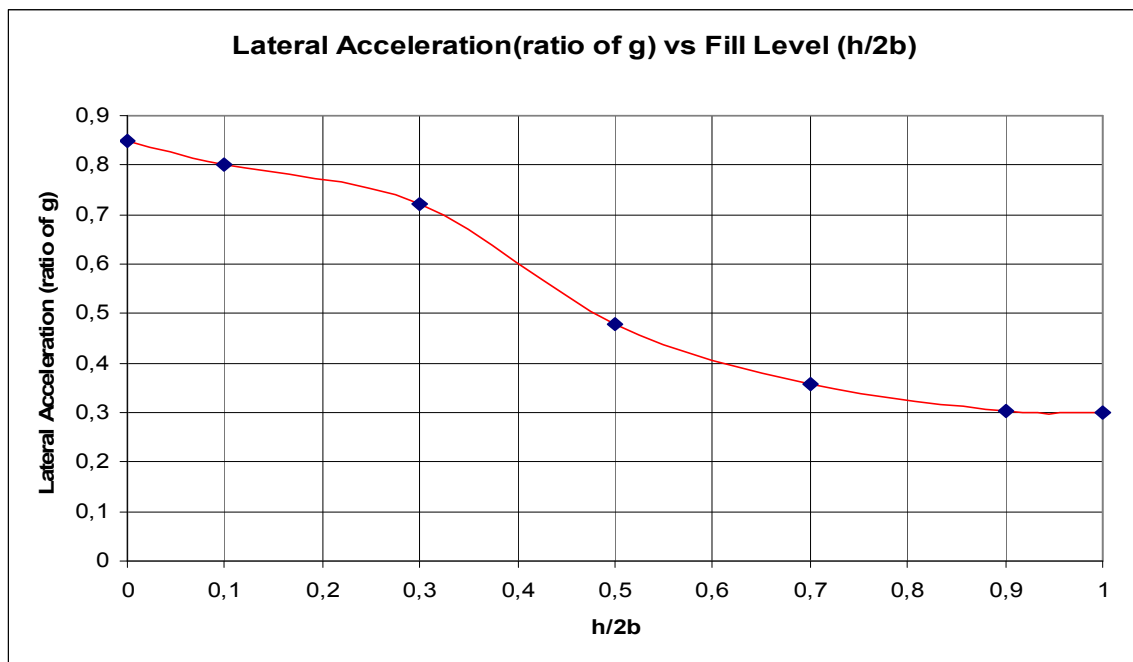


Figure 3.2.8: Plot of lateral acceleration vs fill level for a Clothoid test.

### Lane Change Manoeuvre:

Tests were conducted for different levels of fill and the lateral acceleration were recorded at which rollover took place. Highest accelerations of 0.9g were reached when then fill level were zero. The minimum of 0.3g for a fill level of 100% was found. This threshold varied a lot depending on the fill level similar to the clothoid test. The time period of input oscillation was given as 3 seconds which is very close to the natural frequency for a 50 % fill level at 75 degree initial pendulum angle. For a fill level of 50% the following plots were recorded.

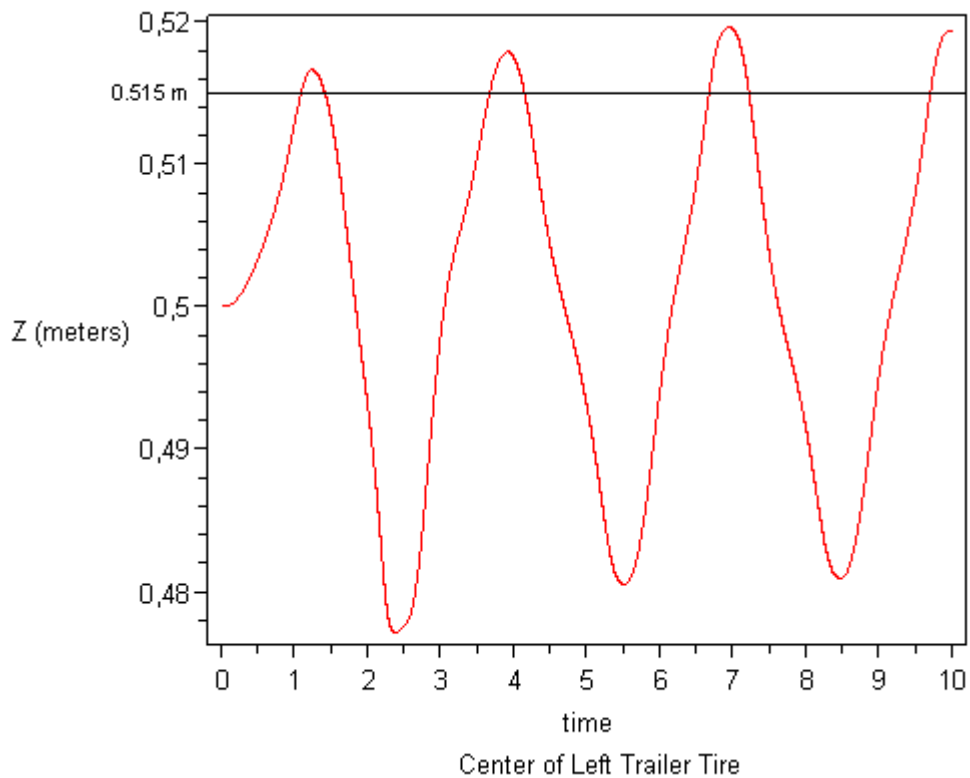


Figure 3.2.9: Vertical displacement of center of left tire during a Lane Change manoeuvre.

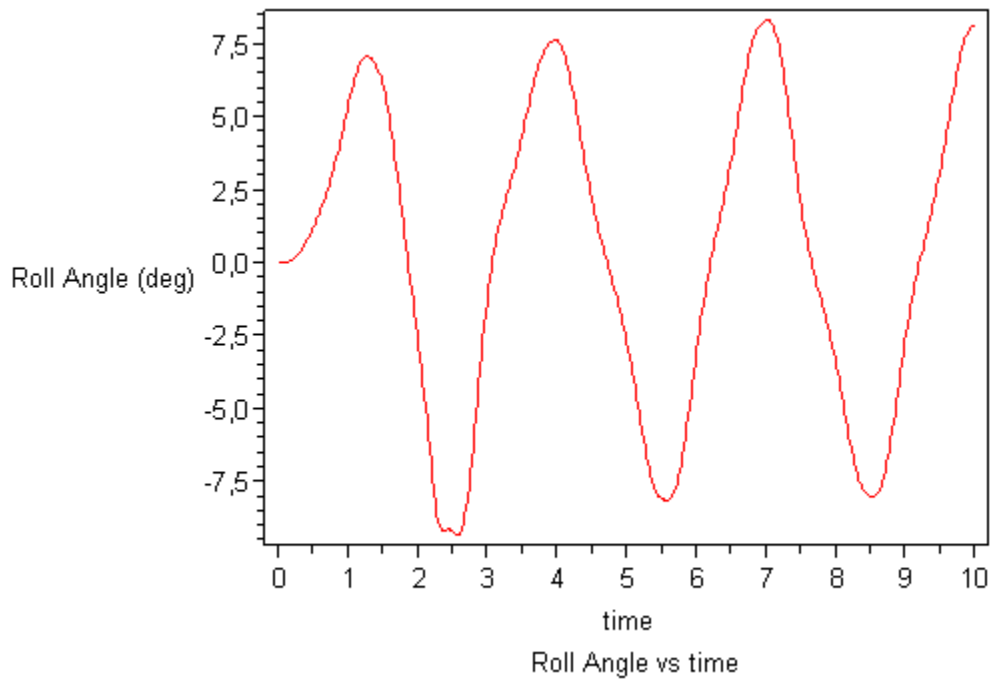


Figure 3.2.10: Change of roll angle vs time during a Lane Change Manoeuvre.

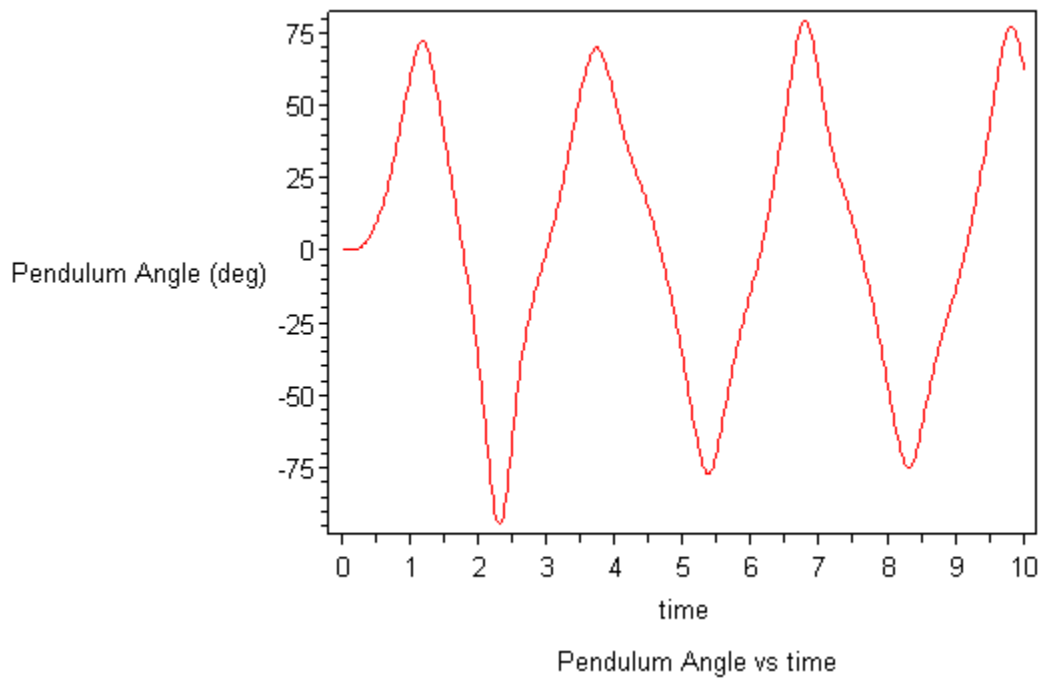


Figure 3.2.11: Change of Pendulum angle vs time during a Lane Change Manoeuvre.

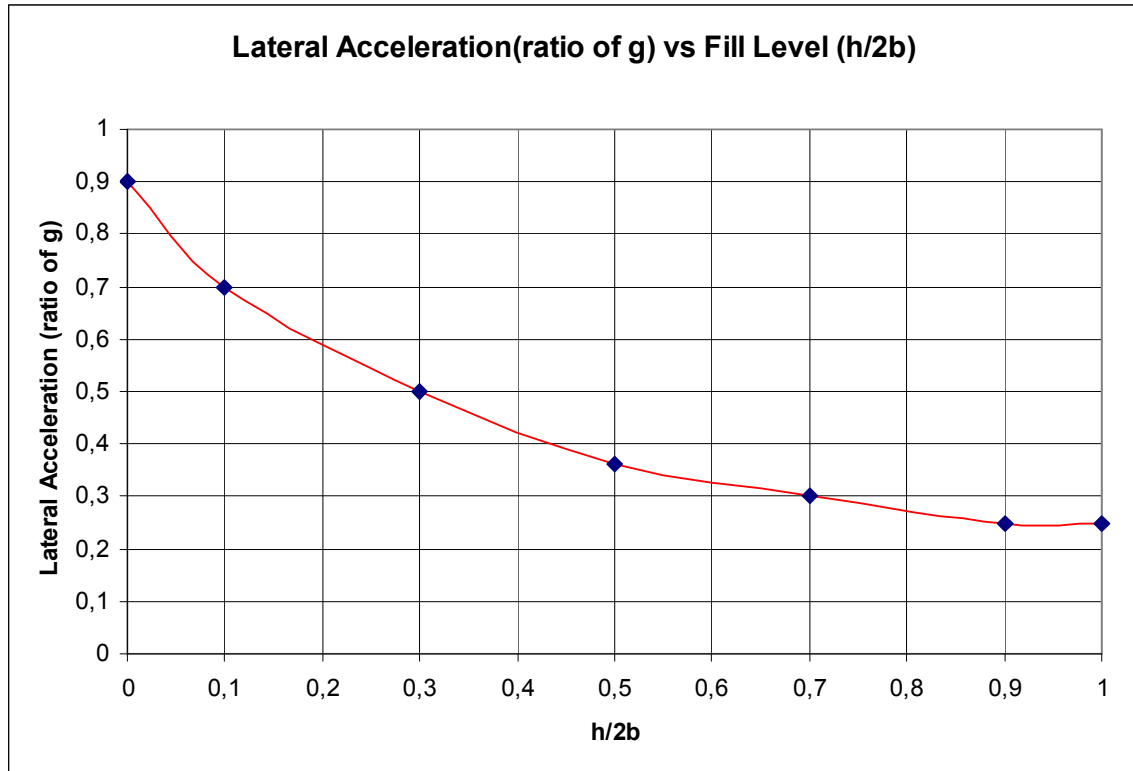


Figure 3.2.12: Plot of Lateral Acceleration vs Fill Level for Lane Change Manoeuvre.

The 2-D model showed results with a large range (0.9g – 0.25g) which includes the rollover thresholds found in the literature. Thus in order to improve the results more complex 3-D models were created which are shown ahead

The Maple code for the model and the simulation can be found in the appendix [2].

### 3.3 Modelization of Trailer

The next step was to create a 3-D Model of the vehicle to get a better representation of the physical model. A right hand coordinate system was chosen with x coordinate as the forward direction, y coordinate as the lateral direction and z coordinate as the vertical direction. The following diagram gives a better understanding of the system modeled and the coordinate system chosen.

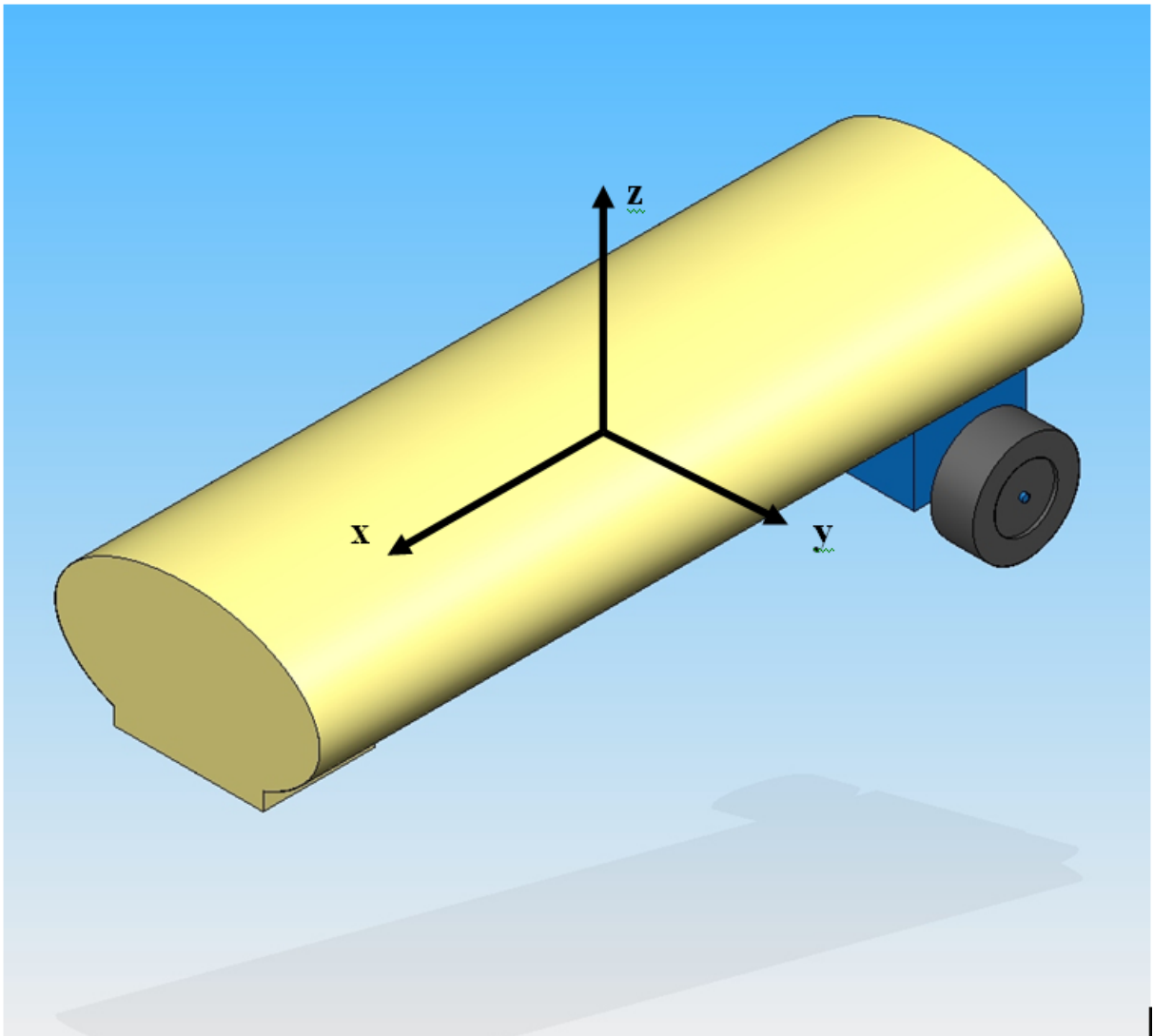


Figure 3.3.1: A 3 dimensional picture of the simplified Tanker modeled showing the coordinate system used.

The semi-trailer model can be described as 11 degree of freedom system. The basic components of the trailer are the cistern, trailer suspension, Left tire, Right tire and the trammel pendulum. The Cistern had 6 degrees of freedom which included translation in the 3 coordinates (forward –  $x$  axis, lateral –  $y$  axis and vertical -  $z$ -axis) and the pitch, yaw and roll motions. The fifth wheel was modeled as a spherical joint between the cistern and the tractor. This was the only joint between the tractor and the trailer making the motion of this point the driver for the trailer. The cistern was connected to the trailer suspension by means of prismatic joint in the  $z$  direction with a spring and damper. The cistern could rotate about the  $x$  axis (the *roll axis*) fixed in the trailer suspension. The location of the roll axis is dependent on the kinematic properties of the trailer suspension and tire compliances. The trailer suspension could also rotate in roll relative to the cistern, enabling the effect of the vertical compliance of the tires on the roll performance to be included in the model. The cistern could also translate vertically relative to the trailer suspension by means of prismatic joints in the vertical direction. This brought the effect of vertical vibration of the cistern relative to the ground.

The suspension springs, dampers, roll stiffness and roll dampers generate moments between the cistern and suspension in response to roll motions and vertical translation. The trailer tires were simplified as single tires on the left and right which had the characteristics of the equivalent 4 tires. The tires were modeled with the *DynaFlexPro* Tire Fiala model. The tires produce lateral forces that vary according with slip angle. The effects of aligning moment, camber thrust, roll steer and rolling resistance generated by the tires were all given by the Fiala model which were automatically generated by the *DynaFlexPro/Tire* package.

The roll stiffness and damping of the vehicle suspension systems were assumed to be constant for the range of roll motions considered. The nonlinear effects of vertical tire stiffness and suspension properties on the stability and performance of the system were neglected. The cistern was considered as a rigid body whose mass and inertial characteristics could be found from the literature. Previous investigations into the roll stability of trailers have all used the assumption the cistern to be a rigid body. However, torsional compliance of the cistern frame influences the distribution of roll moments between axle groups, and significant frame compliance might be expected to affect roll



and handling performance. These effects could have been modeled by using the flexible beam feature of *DynaFlexPro* but as the effects are very small it was neglected.

The trammel pendulum was attached at the center of the elliptical cistern which differs from the c.g. of the trailer body. The trailer body consists of cistern along with some additional accessories like trailer bed for the reinforcements and attachment of the cistern with the suspension. The parameters of the trammel pendulum varied according to the fill level which has already been shown before. The figure shows the Model for the Tanker created in *DynaFlexPro*.

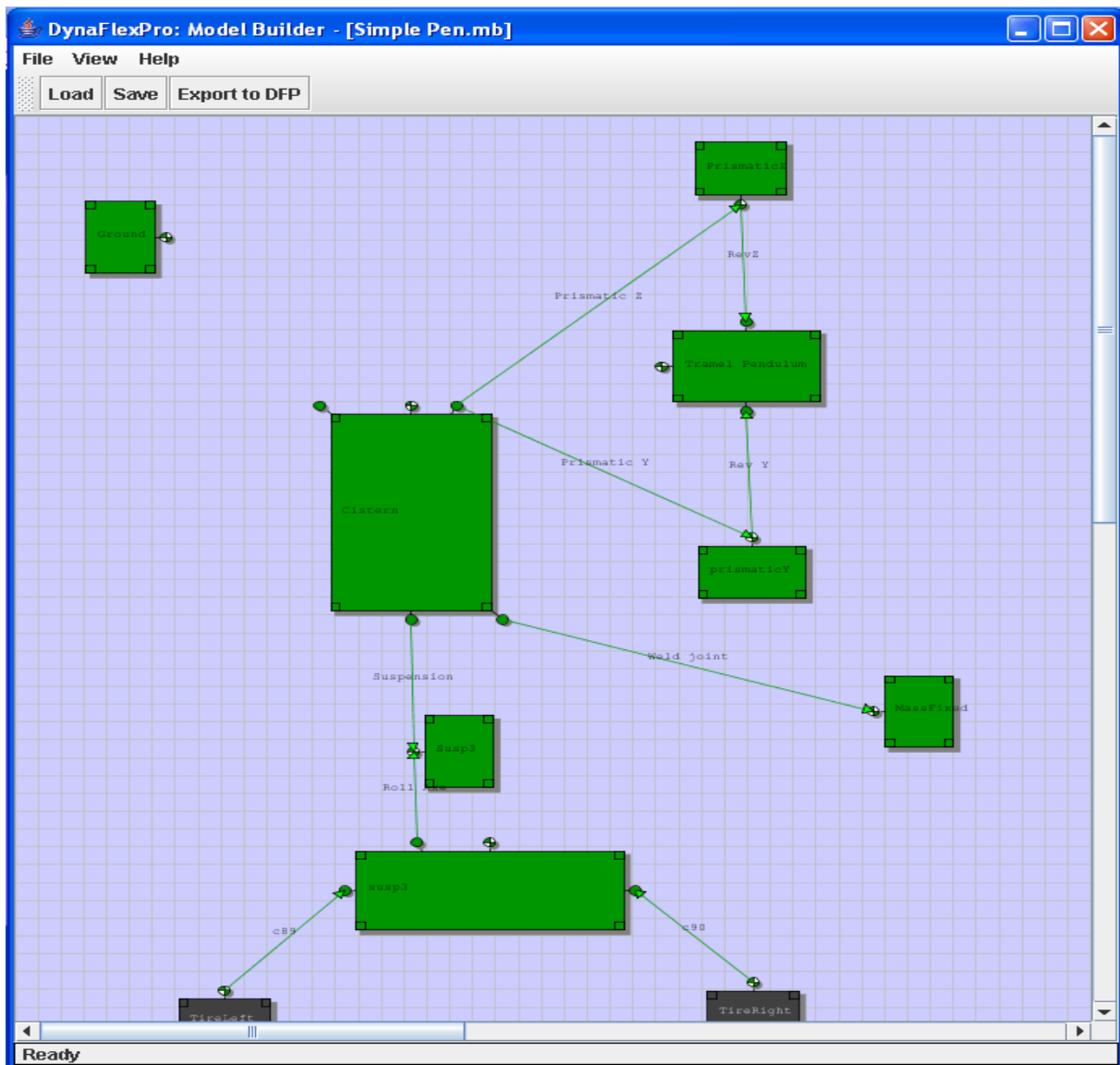


Figure 3.3.2: The *DynaFlexPro* model for the Tanker coupled with the Trammel pendulum.

The calculation of masses of the trailer suspension, cistern and tire are shown below.

$$\begin{aligned}\text{Mass of Suspension} &= 2 * \text{Mass of axles} + 4 * (\text{mass of wheels} + \text{mass of hubs and drums}) \\ &= 2 * 145 + 8 * (37.2 + 39.7) = 905 \text{ kgs.}\end{aligned}$$

$$\text{Mass of Tires (single-left and right)} = 4 * 50.3 = 201.2 \text{ kgs}$$

$$\text{Mass of Cistern} = 6,300 - (905 + 2 * 201.2) = 4992.6 \text{ kgs.}$$

The effects of aerodynamic inputs (wind disturbances) and road inputs (cross-gradients, dips and bumps) were also neglected. This system lacked a motion driver or the component which could induce motions on it. This brought the need of modelization of a tractor which was the next step.

### **3.4 Tractor 3-D Model**

The tractor which was modeled was a 3 axle tractor which has been already shown before, consisting of a tractor unit with a twin drive axle, coupled by a fifth wheel coupling to a twin-axle trailer unit. The single unit tractor was modeled using 7 bodies – 1 to represent the tractor chassis mass, one each for the front and rear axles + wheels which are related as the front suspension and rear suspensions and the 4 tires. Multiple axles at the rear of a vehicle unit were simulated by lumping their effects into a single equivalent axle group. The total system of the tractor has 14 degrees of freedom i.e., forward (x axis), lateral transition (y axis), vertical translation (z axis), yawing, rolling, pitching, suspension compression (front and rear), roll angles (front and rear) and the rotations of the four wheels. The picture below gives a better idea of the modelization.

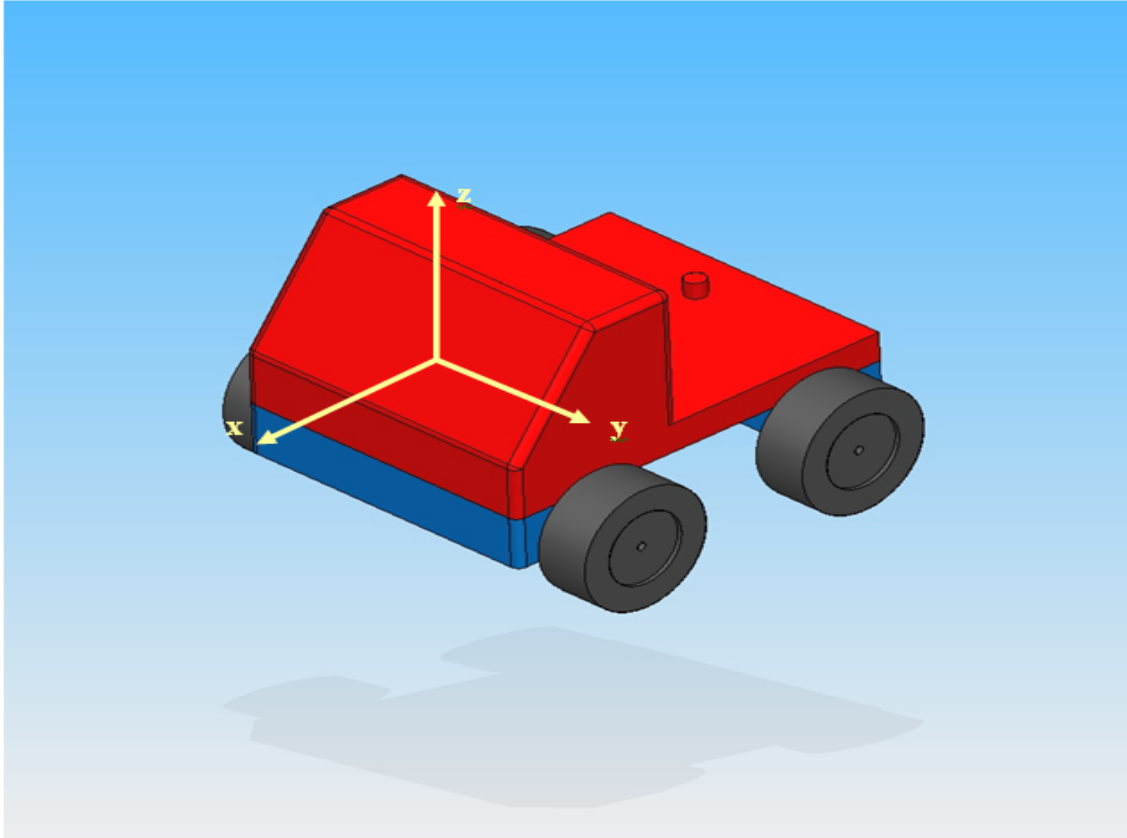


Figure 3.4.1: A 3 dimensional model of the simplified Tractor showing the coordinate system used.

The vehicle as a whole had freedom to translate longitudinally, laterally and vertically and could yaw, pitch and roll. The tractor chassis could rotate about a horizontal axis (the *roll axis front and rear*) fixed in the suspension masses. The location of the roll axis is dependent on the kinematic properties of the front and rear suspensions and tire compliances. The suspension masses could also rotate in roll relative to the tractor chassis, enabling the effect of the vertical compliance of the tires on the roll performance to be included in the model. The tractor chassis could also translate vertically relative to the suspensions by means of prismatic joints in the vertical direction in both the front and rear suspension. This brought the vertical vibration of the chassis relative to the ground.

The suspension springs, dampers, roll stiffness and roll dampers generate moments between the tractor chassis and suspensions in response to roll motions. The tires were modeled with the *DynaFlexPro/Tire* Fiala model. The tires produce lateral forces that vary according with slip angle. The effects of aligning moment, camber thrust,

roll steer and rolling resistance generated by the tires were all given by the Fiala model which were automatically generated by the *DynaFlexPro/Tire* package.

The model was given an initial velocity and steer was given after a few seconds which enabled the model to statically settle on the ground. Individual steer motions could be given to the left and right tires in the front axles and this distribution was according to the Ackerman steer angles.

The roll stiffness and damping of the vehicle suspension systems were assumed to be constant for the range of roll motions considered. The nonlinear effects of vertical tire stiffness and suspension properties on the stability and performance of the system were neglected. The tractor chassis was considered as a rigid body whose mass and inertial characteristics could be found from the literature. The effects of aerodynamic inputs (wind disturbances) and road inputs (cross-gradients, dips and bumps) were also neglected. The model used for simulation created in *DynaFlexPro* is shown below.

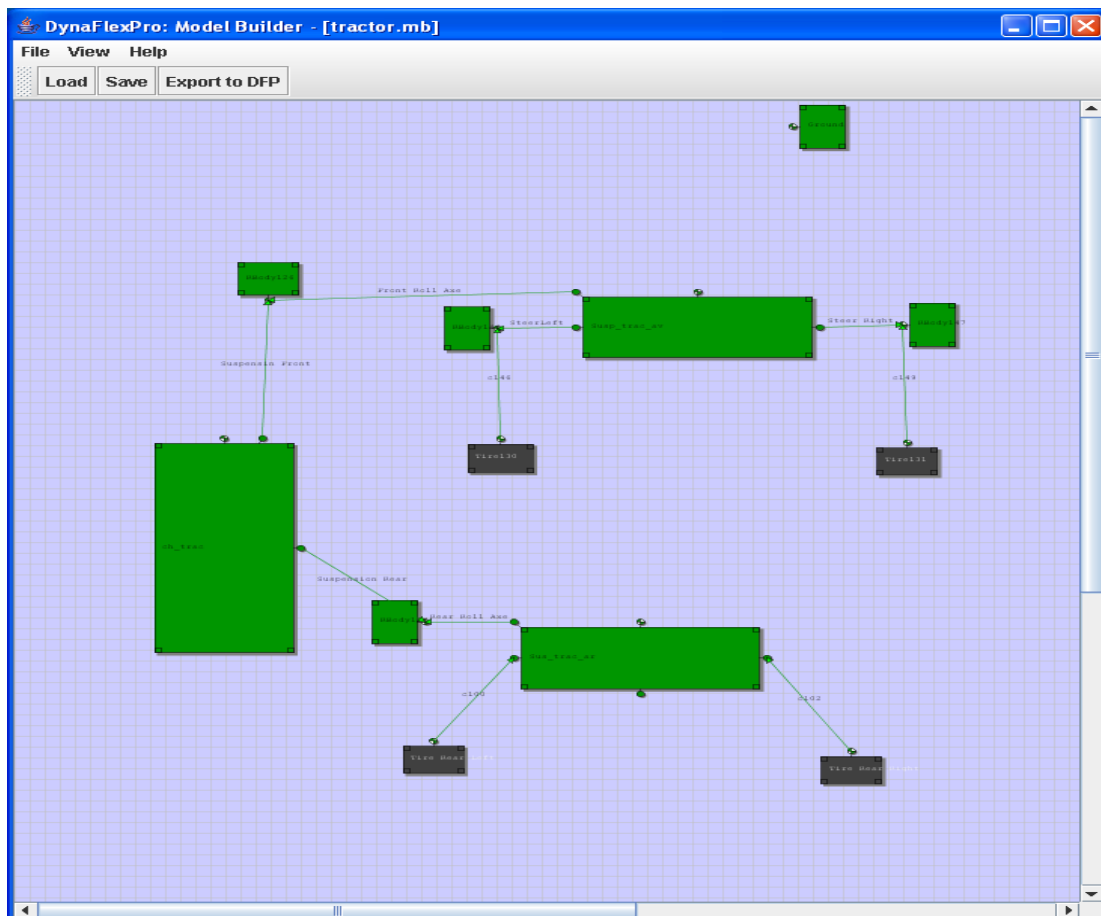


Figure 3.4.2: The *DynaFlexPro* of the Tractor

The calculation of masses of the tractor front suspension, tractor rear suspension, chassis and tires are shown below.

Mass of Front Suspension = 1\*Mass of axles + 2\* (mass of wheels + mass of hubs and drums)

$$= 1*145 + 2*(37.2 + 39.7) = 298.8 \text{ kgs.}$$

Mass of Rear Suspension = 2\*Mass of axles + 8\* (mass of wheels + mass of hubs and drums)

$$= 2*145 + 8*(37.2 + 39.7) = 905 \text{ kgs.}$$

Mass of Tires (front-left and right) = 1 \* 50.3 = 50.3 kgs

Mass of Tires (rear-left and right) = 4 \* 50.3 = 201.2 kgs

Mass of Chassis= 12,000 – (905 + 298.8 + 2\*(50.3 + 201.2)) = 10,293.3 kgs.

### 3.5 Problems with assembly of Tractor and Trailer

Once both the tractor and the Trailer were modeled, basic tests were simulated to verify the system integrity. Once this was validated the next step was to couple the tractor and trailer as a single system. The tractor model was a system with 14 degrees of freedom generalized in 16 variables of equations. The Trailer on the other hand had 11 degrees of freedom with 13 variables. These two systems when coupled together gave a system with 22 degrees of freedom, modeled using 26 generalized coordinates. This system was very complex so there were a number of problems which appear:

- Due to the complexity of the model the option of using “Simplify” in the command *BuildEQs* could not be used. Using this option simplifies the equations of motion making it easier to generate the procedure for simulation. Moreover not only does it give simplified equations but also saves time during using commands like “*GetFrameMotion*”.
- Simulation of this system took huge amounts of time due to some discontinuous and piecewise input functions. The reason was found that using a piecewise function changes the default solving environment to software float environment which is slower. Thus the “dsolve” procedure was forced to work in hardware float environment which is faster. The simplification of these functions and forcing to hardware float environment did reduce the time considerably but still needed some improvements.

With the help of the support members of *DynaFlexPro* ([support@motionpro.ca](mailto:support@motionpro.ca)) these problems were solved but due to some time constraints the changes could not be implemented.

### 3.6 Simplified Model –Trailer with Trammel pendulum

Due to the problems faced during the coupling of the Tractor and Trailer models a simplified approach was followed. It is seen from previous investigations and literature reviews that the tractor is designed to be much more stable compared to the trailer. For simple manoeuvres like cornering, stability of a tractor trailer combination is lost mainly because of the low roll stability of Trailer. Also it can be seen that the motion induced by the tractor on the trailer rests mainly on the forward and lateral directions. Only vibrations of very small amplitude are transmitted to the trailer. Thus it can be safely assumed that the tractor can be simplified to a simple motion driver on the  $X$  and  $Y$  plane. These characteristics of the trailer were confirmed by performing similar tests on the Tractor model alone. The following plot shows the vertical displacement of the point of articulation with the Tanker with respect to time for a clothoid test simulated on the tractor. It can be seen that the maximum vertical displacement is only 0.007 meters which validates the planar motion of the point of articulation.

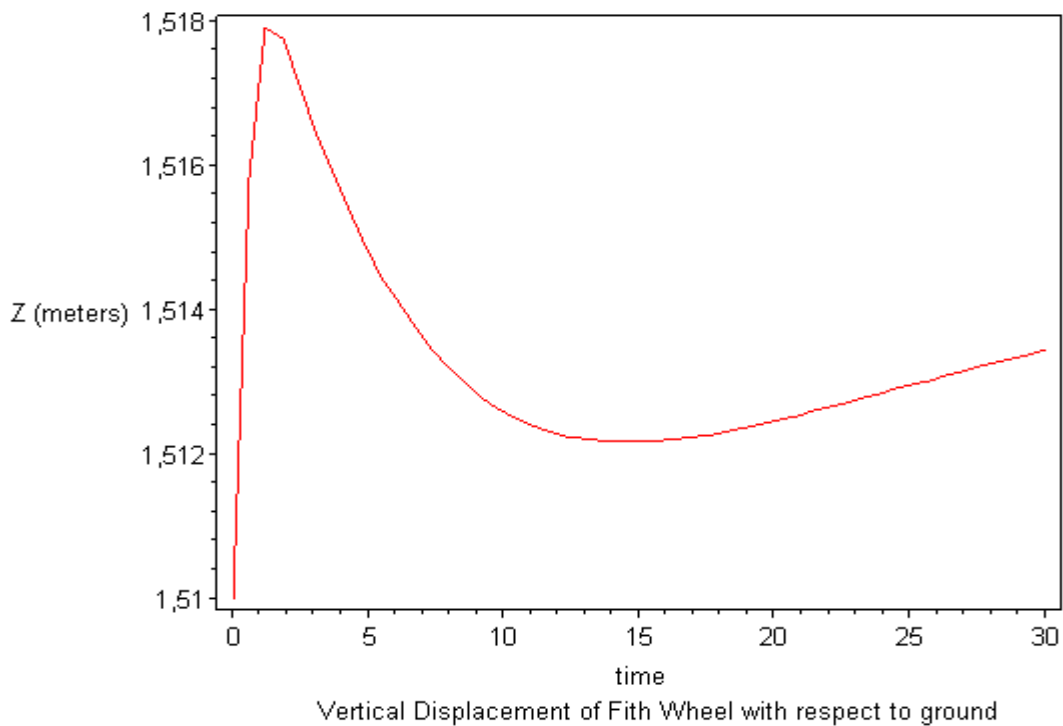


Figure 3.6.1: Vertical displacement of the point of articulation with the Tanker for a clothoid test at 72 km/hr.

Thus the tractor model was replaced by a motion driver to which different displacements in x, y and z axis could be given in functions of time. The following diagram shows the Tanker model with the driver block attached.

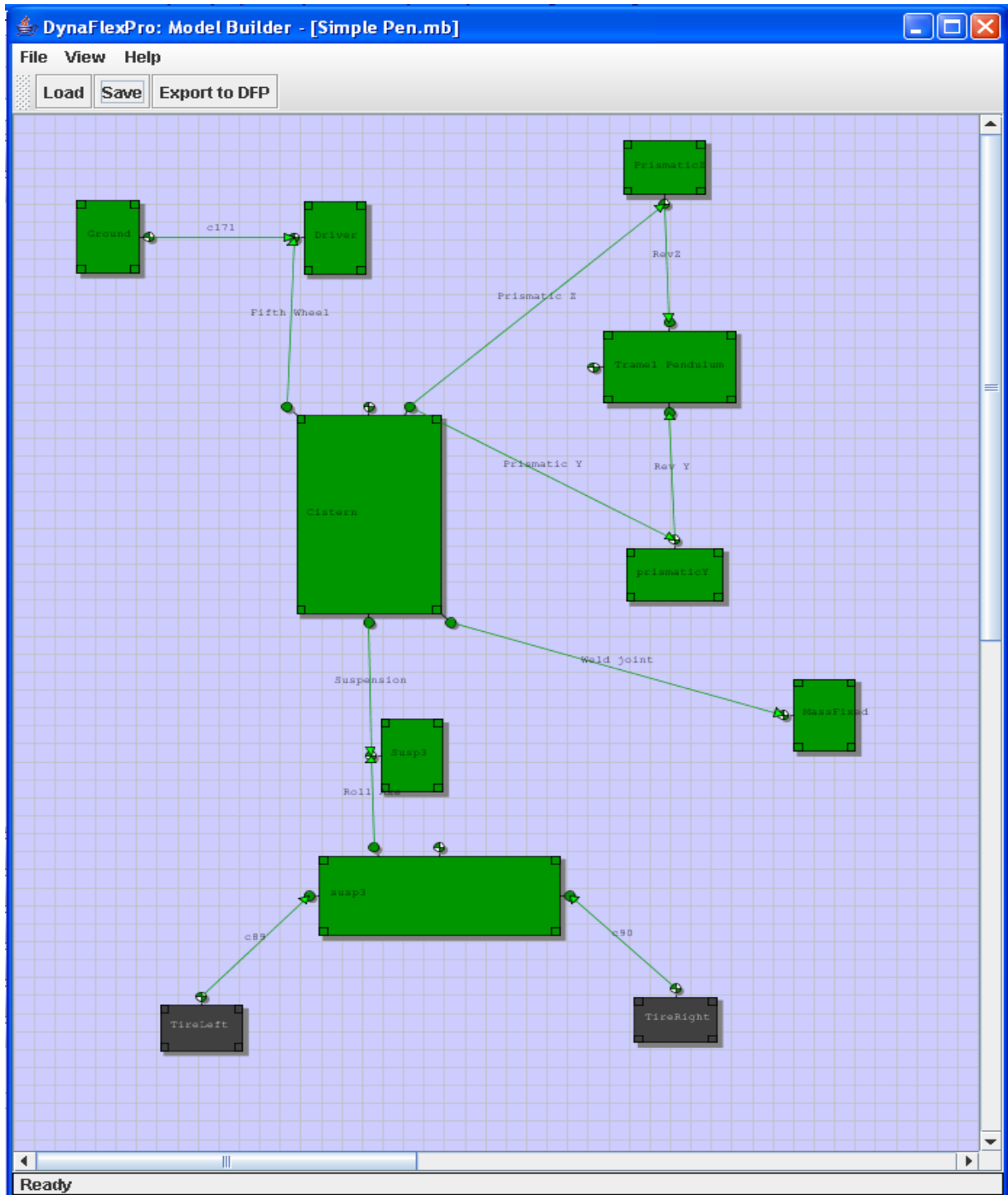


Figure 3.6.2: The *DynaFlexPro* of the Tanker with the Driver model attached.



With this simplified system the following tests were conducted and results were analyzed.

### **Clothoid Test:**

As driver block took only functions of X, Y and Z i.e. in the global reference frame, the parametric equations of the clothoid were found in functions of time. The parametric equations of a clothoid are given by:

$$\begin{aligned} X(s) &= \int_0^s \cos(As^2) ds \\ Y(s) &= \int_0^s \sin(As^2) ds \end{aligned} \quad (3.6.1)$$

One of the constraints in formulating the curve was that the net velocity of the vehicle along the curve remains constant i.e.

$$V_x^2 + V_y^2 = V^2 \quad (3.6.2)$$

Taking  $V_x = \frac{dX(s)}{dt}$  and  $V_y = \frac{dY(s)}{dt}$  equation (3.6.2) was solved to get

$$s = Vt \quad (3.6.3)$$

To find the value of A the property of curvature ( $\kappa$ ) for a clothoid was used.

$$\kappa = \frac{y''}{(1 + y'^2)^{3/2}} \quad (3.6.4)$$

$$\kappa = \kappa_c \frac{t}{T} \text{ for a clothoid} \quad (3.6.5)$$

Using these equations the value of  $A = \frac{\kappa_C}{2VT}$  was found.

For the first 10 seconds the vehicle was given a constant velocity for stabilization. Using these equations the parametric functions of X and Y was found to be:

$$\begin{aligned} t < 5 &\Rightarrow X(t) = 20t \\ t \geq 5 &\Rightarrow X(t) = 100 + V \int_0^t \cos\left(\frac{VKct^2}{2T}\right) dt \end{aligned} \quad (3.6.6)$$

$$\begin{aligned} t < 5 &\Rightarrow Y(t) = 0 \\ t \geq 5 &\Rightarrow Y(t) = V \int_0^t \sin\left(\frac{VKct^2}{2T}\right) dt \end{aligned} \quad (3.6.7)$$

Using these functions the simulations were conducted in order to find the rollover threshold. Though actual rollover takes place at very high values of lateral acceleration, loss in roll stability can be considered when the tire just leaves the ground or when the vertical displacement of the center of tire is just equal to the initial radius of the tire.

The following plots show the different parameters during loss of roll stability of the trailer at 50 % fill level. It can be seen from figure 3.6.3 that after the 0.515 m mark there is a sudden rise showing the overturning of the tanker. The roll angle reaches a maximum of 6 degrees. The lateral acceleration increases linearly as expected during a clothoid test.

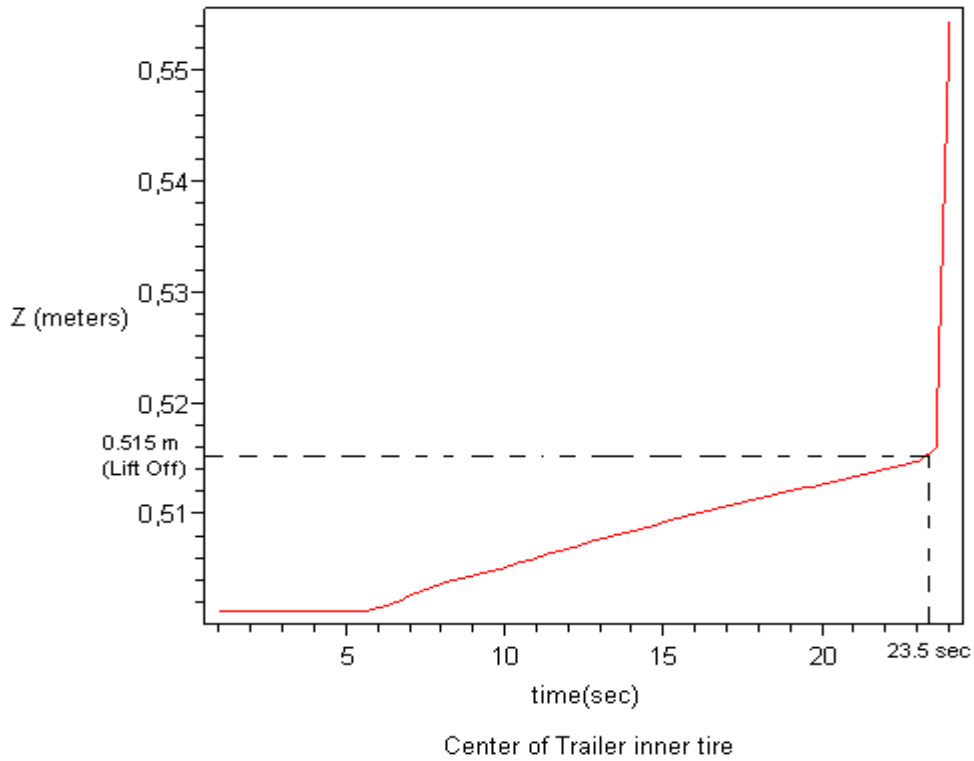


Figure 3.6.3: Vertical displacement of the center of tire with respect to the ground during a clothoid test at 50% fill level.

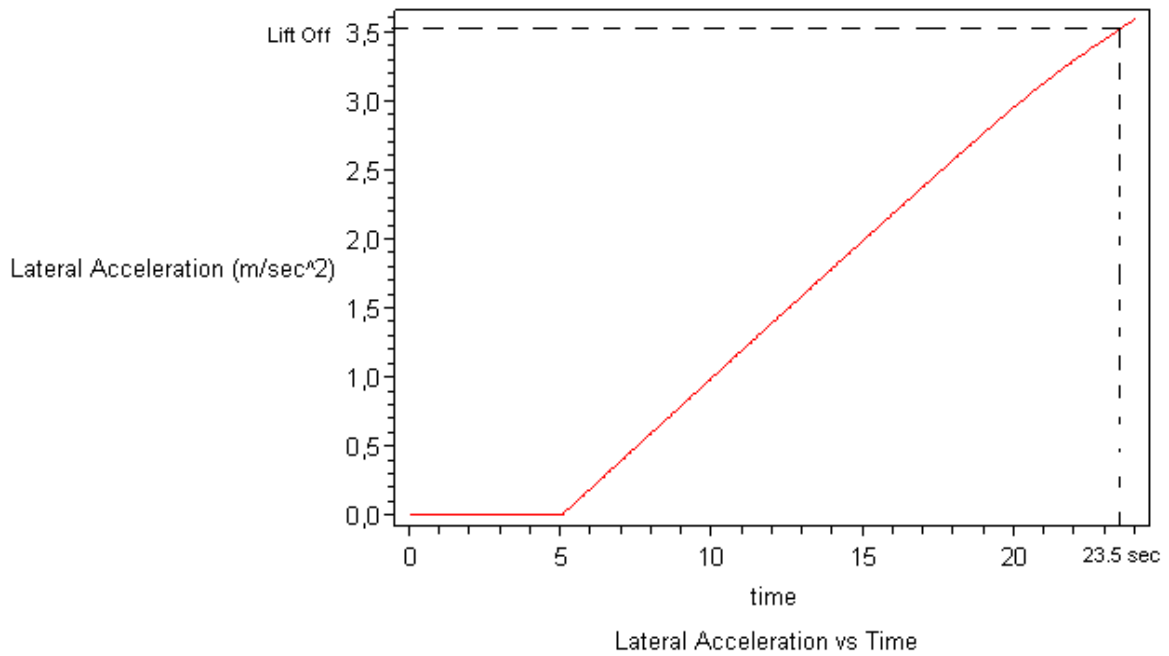


Figure 3.6.4: Lateral Acceleration during a clothoid test at 50% fill level.

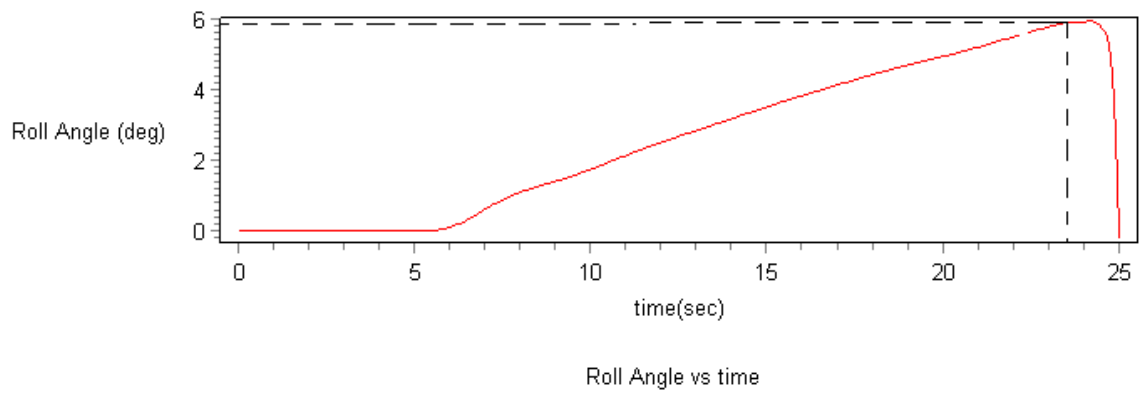


Figure 3.6.5: Roll angle during a clothoid test at 50% fill level.

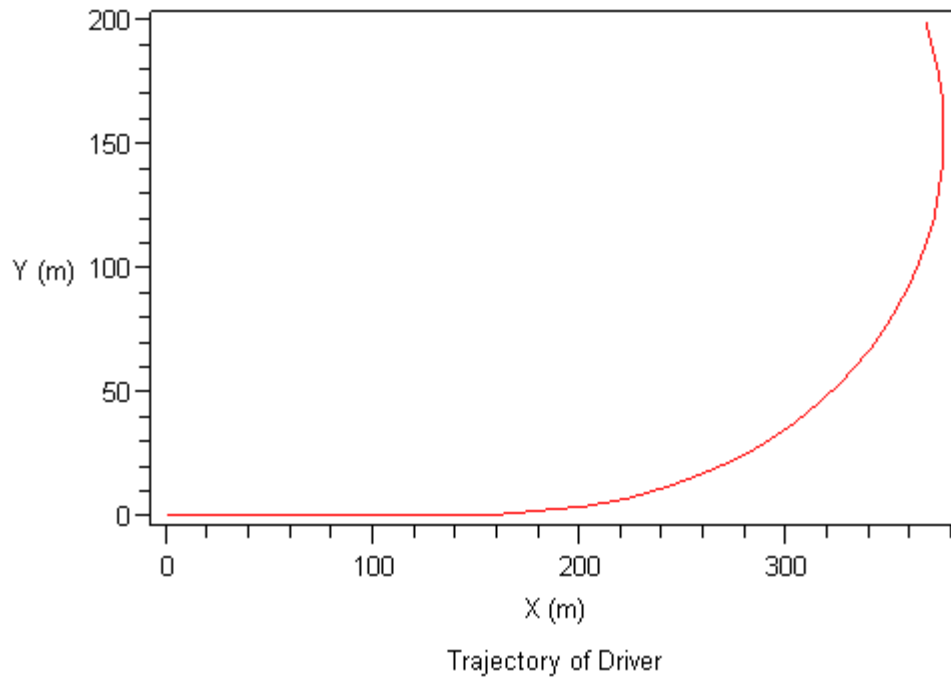


Figure 3.6.6: Trajectory of driver during a clothoid test at 72 km/hr.

Tests were conducted at different fill levels and lateral acceleration at which rollover took place was noted. The following plot shows the variation of lateral acceleration with respect to fill level. A sudden decrease in values around the 50% mark can be seen showing the effect of sloshing.

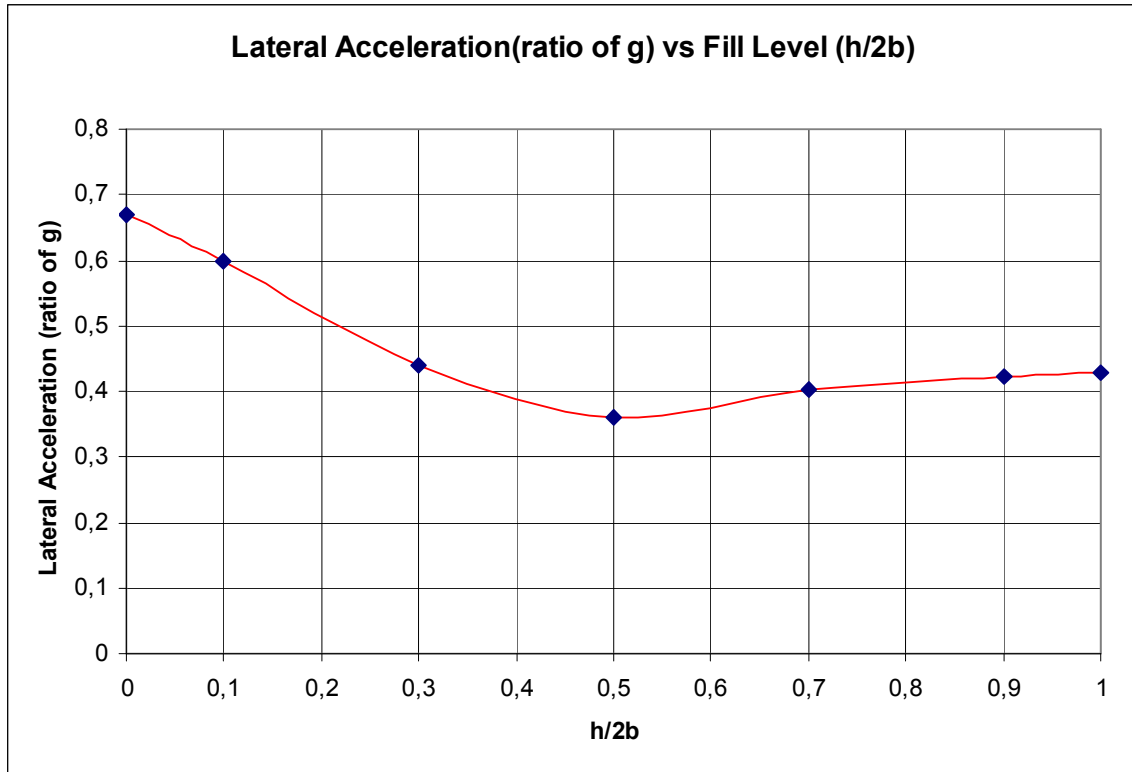


Figure 3.6.7: Lateral Acceleration vs fill level for a clothoid test at 72 km/hr.

## CHAPTER FOUR

### CONCLUSIONS AND DISCUSSION

With the number of algorithmic and computational advances, Multi-body Computer-Aided Engineering (MCAE) tools for analyzing evermore complex multibody systems have increased making it easier to automate and simplify the modeling and analysis of multibody system performance, well-known examples include DADS, ADAMS, Working Model, visual-NASTRAN, and SD/FAST. But all these tools have limitations making it very difficult to choose the best for our purpose. Some of these limitations are stated below. Firstly, the general-purpose formulations can introduce numerical approximations and thus errors in subsequent numerically based solutions. Second, models created with most MCAE tools are unsuitable for real-time implementation. Further, models might be difficult to parameterize using dynamic system characteristics, such as masses or inertias as opposed to more traditional geometric characteristics such as lengths that are prevalent in MCAE systems.

DFP is a new MCAE tool that exploits Maple's symbolic manipulation power for automatically creating the governing Equations of Motions for large mechanical multibody systems in symbolic form. The parametric nature of the resulting symbolic model makes it well suited for the parametric system-performance studies, for use in design-refinement of such systems, or the development of suitable controllers.

Furthermore, the code generation capability can be used to export the generated model to other platforms such as Matlab, C or Fortran. Thus, engineers seeking to design, analyze, or control a mechanical multibody system can use DFP to efficiently and rapidly derive high-fidelity system-models that are suitable for use in real-time engineering simulators or hardware-in-the-loop testbeds. Few of the features which give *DynaFlexPro* a lead in the competition are given below.

- Models and simulates the motion of multibody mechanical systems be it forward dynamics, inverse mechanics and sensitivity or parametric analysis.
- Java Graphics User Interface for rapid modeling with block diagrams.
- Large library of components, including rigid bodies, flexible beams, joints, springs, dampers, forces and moments.
- User-selected modeling coordinates, including absolute coordinates. Choosing appropriate body and joint elements for the spanning tree allows the user to select the variables that appear in the final EOMs.
- Automatic generation of kinematic and dynamic equations in symbolic form (Maple 10).
- Generates optimized code for real-time simulation.
- *DynaFlexPro* algorithms combine linear graph theory with physical models.
- DFP simplifies modeling of the nonlinear constitutive behavior of components. Using a symbolic form for representation of equations makes it easier for the non linear modeling. For instance, changing the spring constant and damping coefficient properties to ' $k * x(t)^2$ ' allows us to model the nonlinear force-displacement behavior  $F = k * x(t)^3$  of the spring.

An attempt was made to utilize all these features to its best in the 2-D and 3-D modeling of the Heavy Tanker vehicle and the Trammel Pendulum. Firstly, modeling the sloshing effect of liquid in an elliptical tanker by Trammel Pendulum has a number of advantages. One of the main advantages is that the trammel pendulum model is a simple mechanical system which makes it easier to integrate in a rigid body vehicle model. Also compared to a Finite Element model of fluid in a tanker, the trammel pendulum is much simpler to model and as the simulation code is not bulky, there is a considerable decrease in simulation time. Apart from this it can also be mentioned that the trammel pendulum models are much more stable from the numerical stability point of view than fluid models making it easier for study and analysis.

From the modeling it can be seen that for the Trammel Pendulum Model, the natural frequencies obtained from the *DynaFlexPro* Model shown in Figure 2.5.6 were in good correlation with the plots obtained by Salem (Figure 2.5.7). Also the plots for angular positions and angular velocity at different values of initial angle agree with the ones found out by Salem in his work. This validates the model assuring the same effect as that of sloshing in elliptical tanks for small angles of rotation. Also the parameters of the pendulum were set by dynamic comparison with FEM model for small angles of oscillations. This criterion of small oscillations was sufficiently fulfilled by the small roll angles of the models around 5 degrees but at very high lateral acceleration such as 0.5g the Trammel pendulum angle deflected to high values of 50 degrees which is in its non linear regime. This was also observed by Salem in his work and this led him to compare the trammel pendulum behavior beyond the linear range. The comparison showed that the trammel pendulum produced up to 20% more lateral forces and moments than the fluid models beyond the linear range, which renders the pendulum model more conservative from the tanker stability point of view.

The 2-D model of the trailer showed sufficiently conservative results with high lateral accelerations of upto 0.85g for a clothoid test at 0 % fill level and 0.9g for a Lane Change Manoeuvre at 0% fill level where the system acts as a rigid body. Increasing the fill level definitely decreased the rollover threshold as expected with lowest accelerations of 0.3g for a clothoid at 100% fill and 0.25g for a LCM at 100% fill level. There can be two main conclusions which can be drawn from the Lateral Acceleration plots in Figures 3.2.7 and 3.2.11.

Firstly the effect of increasing the fill level increases the height of center of gravity of the system making it more vulnerable to roll over. This is quite expected from general dynamics point of view. Secondly both the plots show a sudden dip at 50 % fill level showing the effect of sloshing considerably. Previous studies have shown that the effect of sloshing increases with increase in fill level till it reaches a maximum at around 50 %– 60 % fill level. After which the effect of sloshing decreases considerably for higher values of fill level. For the 2-D case, though the sudden dip indicates the effect of sloshing there is no rise in rollover threshold for higher fill levels. One of the reasons for



this could be that the decrease in sloshing effect was balanced by the increase in height of c.g. of the system.

Another important conclusion which can be drawn from the results of LCM test (Figures 3.2.8 – Figures 3.2.10) for the 2-D case at 50 % fill level is that the natural frequency at 50 % fill level with initial pendulum angle of 75 degrees matches with the excitation function's time period of 3 seconds. This could also be one of the reasons for the decrease in threshold values around 50% fill level.

For the 3-D case the results seemed to be more realistic. From the results of the clothoid test (Figures 3.6.1 – 3.6.5) it can be seen that the results obtained are very much in correlation with the experimental tests which can be found in literature. The values range from a maximum rollover threshold value of 0.67g at 0% fill level to a minimum of 0.36g at 50 % fill level. From the plots, the effect of sloshing can be clearly visible. The decrease in threshold values around the 50%-60% fill level which has been mentioned earlier is clearly visible. There is a considerable rise in values (till 0.428g for a 100 % fill level) after the 50 % fill level showing the decrease in sloshing effects.

## **CHAPTER FIVE**

### **RECOMMENDATIONS AND FUTRE WORK**

No analysis would be complete without a discussion of the potential limitations and scope-of-use of such software. This discussion is especially pertinent in light of the numerous commercially available MCAE software packages. First, and foremost, there is an assumption that a user has the capability to perform the initial modeling. Suitable selection of frames of reference, generalized coordinates, and other aspects can have a tremendous influence on the resulting form and size of the EOMs. Thus, while the Java GUI facilitates the specification of interconnections in block-diagram form, the user still needs to specify the sequence of interconnections. Second, although the current library of components is reasonably comprehensive, the modeling of certain large multibody systems could pose some challenges to a novice. Third, DFP still does not possess the conveniences that commercial-off-the-shelf packages offer in terms of model creation and simulation. Features such as 3D visualization capabilities, automated mass and inertial calculations are currently missing. Finally, while the automated processing to create the EOMs has been adequately shielded from the user, the user is expected to have a good grasp of Maple programming concepts and data-storage constructs to effectively use the results.

Despite these limitations, *DynaFlexPro* represents the leading edge of rapid symbolic system model generation for high-fidelity performance analysis and control. As such, it is ideally suited for a user who is reasonably well versed with traditional analytical modeling, has encountered the limitations of traditional MCAE packages, and is looking to exploit symbolic modeling in developing real-time engineering models of large multibody systems.

Modeling mechanical systems is an endless work as every model is based on some approximations which make it lag behind the real model. But there is always a possibility to describe it more accurately. The present work was one such attempt to

describe a heavy duty tanker in a better way. However there are some areas which are open for improvement.

- Firstly, attempts should be made to assemble the tractor and tanker 3-D models. Though the model code and equations seem to be very heavy and consume time, simple changes in the input functions and modelization can cause huge decrease in computational time.
- The fluid in the elliptical tanker was modeled as trammel pendulum and a fixed mass, the trammel pendulum to represent the dynamics of the sloshing liquid and the fixed mass to represent the relatively stationary liquid. For lateral accelerations above 0.5g a fluid model shows higher modes of oscillation and the flat liquid surface assumption is no longer valid. Thus an attempt should be made to define the trammel pendulum parameters in the non linear domain.
- Suspension and pneumatic compliances of a vehicle are often nonlinear. These non linear characteristics of the springs and dampers have been ignored in these models. Including these characteristics which is very easy with *DynaFlexPro* might give vehicle model closer to reality.
- The aerodynamic effects which have been neglected should be included as external functions depending on the velocity components of the vehicle which is also very easy to implement with *DynaFlexPro*.

## References

- [1] Anon. *Road Accidents in Great Britain*. Department of Transport, HMSO, UK, 1994.
- [2] Chris Winkler, Rollover of Heavy Commercial Vehicles, UMTRI Research Review, ISSN 0739 7100 October–December 2000, Vol. 31, No. 4
- [3] David J. M. Sampson, David Cebon (2001) *Achievable Roll Stability of Heavy Road Vehicles* Proc. IMechE, Journal of Automobile Engineering, Cambridge University Engineering Department
- [4] Dean Karnopp, *Vehicle Stability*, University of California, Davis
- [5] G. Genta (1997) *Motor Vehicle Dynamics-Modeling and Simulation*
- [6] Heins N. Karam, “DYNAMIC STABILITY OF AN ELLIPTICAL PENDULUM WITH UNILATERAL SIMPLE SUPPORTS”.
- [7] J.R. Ellis (1994) *Vehicle Handling Dynamics*, London, Mechanical Engineering Publications Limited
- [8] J. Christian Gerdes, Paul Yih, Krishna Satyan, *Safety Performance and Robustness of Heavy Vehicle AVCS*, Department of Mechanical Engineering - Design Division Stanford University *California PATH Program, Year One Report for MOU 390, January 2002*
- [9] Rakheja, S., and Ranganathan, R., “Estimation of the Rollover Threshold of Heavy Vehicles Carrying Liquid Cargo: a Simplified Approach,” *Heavy Vehicle Systems, Int. J. of Vehicle Design*, Vol. 1, No. 1, 1993.
- [10] Roman Kamnik, “Roll Dynamics and Lateral Load Transfer Estimation in Articulated Heavy Freight Vehicles: A Simulation Study”
- [11] S. McFarlane, P. F. Sweatman, and J. H. F. Woodroffe. The correlation of heavy vehicle performance measures. *SAE Transactions*, 106(973190):459–465, 1997.
- [12] Salem, M., “Rollover Stability of Partially Filled Heavy-Duty Elliptical Tankers Using Trammel Pendulums to Simulate Fluid Sloshing”, Ph.D. Dissertation Proposal, WVU 1999.
- [13] T.-T. Fu and D. Cebon, *ANALYSIS OF A TRUCK SUSPENSION DATABASE*, *International Journal of Vehicle Design, Heavy Vehicle Systems March, 2002*

- [14] UMTRI Research Review, University of Michigan Transportation Research Institute, October-December 2000, Volume 31, Number 4.

## Appendix:

### [1] Code for Trammel Pendulum Model.

```
> restart:
> with(DynaFlexPro):with(plots):with(plottools):
    "DynaFlexPro - version 2.4.0"
    "Copyright 2005-2007, MotionPro Inc."
    "'DynaFlexPro Tire` components installed."
    "Type '?DynaFlexPro' for help with DynaFlexPro."

>Model:=BuildEQs("D:/Travail/VENU_GORU/examples/project/2dPenTramel.dfp",["D
ynSimpType","none","AugType","Reaction"]);
    "Analyzing system..."
    "Performing constraint analysis..."
"The system has 1 degree(s) of freedom. It is modeled using 3 generalized
coordinate(s) coupled by 2 algebraic constraint(s)."
"Performing a dynamic analysis using an augmented reaction formulation - system
variables shown below:"
    "Dynamic analysis complete."
    "Saving model for future use...: "
"DynaFlexPro unable to save model....cannot lock repository, D:/Travail/VENU_
GORU/examples/project/2dPenTramel.lib"
module () local SetOptions, DFPMModule, Print, vPd, vPd_dot, xJi, xJdInv, xG,
vDepVels, vDepAccels, AnalyseModel, KinAnalysis, DynAnalysis, SetGenCoords,
SetQiQd, SetJacPos, SetJacVel, SetJdInvAndG, SetDepVels, SetDepAccels,
SetQiDepEdgeInfo, GetConstraints, GetSubbedTerm, ModType, lmQiSys, lmQdSys,
lmQiPreSolved, lmQdPreSolved, llmSubSysCons, teVelConstraintInfo,
teZeroReactionSubs, leJdInvSubs, leGSubs, leDepAccSubs, leMFSubs, vPosCons,
vVelCons, vAccCons, vDynEQs, leConstParams, leVarParams, leReParamSubs,
bSolvePosition, bSubMF, sDynSimpType, sKinSimpType, bSubEmbed, bSimpEmbed,
sAugType, sFormType, leBaumgarte, bGenSubSys, bSilentMode, mLGM, mMath,
```

```
pTFunc, sModType; export GetParams, GetInputs, GetPosCons, GetVelCons,
GetAccCons, GetDynEQs, GetKinTrans, GetSysEQs, GetSysODEs, GetAYBSysODEs,
GetFrameMotion, SetBaumgarte, GetSimCodeData, GetLGM, GetMass, GetCoM,
GetInertia, Reparameterize, sDFPVersion, sLibFile, vQ, vQdot, vP, vPdot, vX, vXdots,
vKinTransRHS, xJacPos, xJacVel, vVelRHS, vAccRHS, xM, vLambda, xC, vF,
vReactions, mExprMan; option package; end module
```

```
> with(Model);
```

```
[GetAYBSysODEs, GetAccCons, GetCoM, GetDynEQs, GetFrameMotion, GetInertia,
GetInputs, GetKinTrans, GetLGM, GetMass, GetParams, GetPosCons,
GetSimCodeData, GetSysEQs, GetSysODEs, GetVelCons, Reparameterize,
SetBaumgarte, mExprMan, sDFPVersion, sLibFile, vAccRHS, vF, vKinTransRHS,
vLambda, vP, vPdot, vQ, vQdot, vReactions, vVelRHS, vX, vXdots, xC, xJacPos,
xJacVel, xM]
```

```
> parasubs:=[G=9.81,
```

```
> a=2.4/2,b=1.219/2,fill=0.5,liquidfull=22000,
```

```
> hFill=fill*2*b,
```

```
> xh=a*(2*hFill/b-(hFill/b)^2)^0.5,
```

```
m_Fix = 525.57195,
```

```
m_pen = 4022.588066,
```

```
abar = .2293779290,
```

```
bbar = .1165048731,
```

```
> hFix1=(ycg-m_pen/mtot*(1-bbar/b))/(1-m_pen/mtot),
```

```
> hFix=b-hFix1,F=0
```

```
> ];
```

```
> GetDynEQs():GetPosCons();
```

```
> BuildSimCode(Model,{"Xdots"},"MapleProc","Optimize",[op(parasubs)]);
```

```
"-----Processing Xdots-----"
```

```
> odeVars := convert(convert([Model:-vX],Vector),list);
```

```

> ICs:=array([0,0,0,a,ang*Pi/180,ang*Pi/180]);
> tr := time():
SolnXdot:= dsolve(numeric, implicit=false, procedure=pXdot, abserr = 1e-8, relerr=1e-7,
start=0, initial=ICs, output=listprocedure, procvars= odeVars, range=0..50):
Time_to_integrate := time()-tr;
> zP(t):= GetFrameMotion("r","cgPen","mGND","mGND",parasubs)[3];
> yP(t):= GetFrameMotion("r","cgPen","mGND","mGND",parasubs)[2];
>plots[odeplot](SolnXdot,[eval(yP(t)),eval(zP(t))],t=0..50,numpoints=500,scaling=constrained);
>plots[odeplot](SolnXdot,[t,odeVars[3]*180/Pi],t=0..20,numpoints=500,scaling=constrained, title= "Angular Velocity(deg/sec) vs time at 150 degrees initial angle", labels= ["time(seconds)", "theta_dot(deg/sec)"]);
>plots[odeplot](SolnXdot,[t,odeVars[6]*180/Pi],t=0..20,numpoints=500,scaling=constrained, title= "theta vs time at 150 degrees initial angle", labels= ["time(seconds)", "theta(deg)"]);
> cordinate:=proc(point,time)
local v1,v2,v3,v4,v5,cord;
v1:= rhs(SolnXdot(time)[5]):
v2:= rhs(SolnXdot(time)[6]):
v3:= rhs(SolnXdot(time)[7]):
cord:=eval(GetFrameMotion("r",point,"mGND","mGND",parasubs),[sH(t)=v1,theta_H(t)=v2,theta_V(t)=v3]);
end:
> cordinate("cgPen",0)[2];
> anim:=proc(time,n)
local i,l,frame,step,c,cH,cV,gndH,gndV;
step:=time/n;
gndH:=line([-3,0],[3,0],colour=black,thickness=1);
gndV:=line([0,-3],[0,3],colour=black,thickness=1);
for i from 0 to time*n do

```



```

c[i]:=circle([cordinate("cgPen",i*step)[2],cordinate("cgPen",i*step)[3]],0.1,color=blue,thi
ckness=2):
cV[i]:=circle([cordinate("pV",i*step)[2],cordinate("pV",i*step)[3]],0.02,color=black,thic
kness=2):
cH[i]:=circle([cordinate("pH",i*step)[2],cordinate("pH",i*step)[3]],0.02,color=black,thic
kness=2):
l[i]:=line([cordinate("pV",i*step)[2],cordinate("pV",i*step)[3]],[cordinate("cgPen",i*step
)[2],cordinate("cgPen",i*step)[3]], color=red,thickness=2):
frame[i]:= display({gndV,gndH,c[i],l[i],cV[i],cH[i]});
od:
display([seq(frame[i],i=0..time*n)],insequence=true,scaling=constrained,axes=none);
end:
> anim(2,100);

```

## [2] Code for 2-D Model.

```

> restart;
> with(DynaFlexPro);with(plots);
      "DynaFlexPro - version 2.4.0"
      "Copyright 2005-2007, MotionPro Inc."
      "'DynaFlexPro Tire` components installed."
      "Type '?DynaFlexPro' for help with DynaFlexPro."
[Activate,  BuildEQs,  BuildModel,  BuildSimCode,  GetDFPdir,  GetModel,
  SaveModel,SetOutputDir,  Version,  mConstants,  mConstructors,  mLibMan,
  mStoreFileMan]
>Model:=BuildEQs("D:/Travail/VENU_GORU/examples/project/2dPnuTrammel.dfp",["
  DynSimpType","Simplify"]);
      "Analyzing system..."
      "Performing constraint analysis..."
      "The system has 3 degree(s) of freedom.  It is modeled using 5 generalized

```

```

coordinate(s) coupled by 2 algebraic constraint(s)."
"Performing a dynamic analysis using an augmented lagrange formulation -
  "Dynamic analysis complete."
    "Saving model for future use...: "
      "DynaFlexPro unable to save model....cannot lock repository, D:/Travail/VENU_\
        GORU/examples/project/2dPnuTrammel.lib"
> with(Model);GetParams();
> parasubs:=[Clat=100000, Clong=100000, Crr=0,r2=0.572/2, G=9.81,mu1=1, mu2=1,
f=0.66,
Ixxc=5000*f,
Ixxp=(750+2*n3*30),
tp=1.05,hr3=0.24,hp=0.3, ps3=1.285-hr3,
R=0.5,
K_Roue=870000,D_Roue=100000,
KSusp3=1800000,Krot3=850000,
DSusp3=350000,Drot3=35000*3,
m_Cit=5000*f,
m_Susp3=908+400,
n2=4,n3=4,
a=2.4/2,b=1.219/2,fill=1,pa=0.7396,liquidfull=22000,
hFill=fill*2*b,
ti=19,
#Trammel Pendulum Parameters @ 50%,
hFix = 0.0727383943-hp,
m_Fix = 2801.344824*f,
m_pen = 8198.65516*f,
abar = 0.634381521,
bbar = 0.3222129477,
mtot = 11000*f,
IxxPen=1,IyyPen=1,IzzPen=1,

```

```

IxxFix=m_Fix/mtot*18300,IyyFix=m_Fix/mtot*183000,IzzFix=m_Fix/mtot*183000,H=
    1.555,
#F=piecewise(t<ti,0.04*G*t,t>=ti,0.04*G*ti)
F=0.36*G*sin(2*Pi*t/3)];
> BuildSimCode(Model,{"Xdot"},"MapleProc","Optimize",[op(parasubs)]);
    "Order of the State Variable Array: "
> tr := time();
    SolnXdot:= dsolve(numeric, implicit=false, procedure=pXdot, abserr = 1e-8, relerr=1e7,
        start=0, initial=ICs, output=listprocedure, procvars= odeVars, range=0..50):
Time_to_integrate := time()-tr;
>plots[odeplot](SolnXdot,[t,GetFrameMotion("r","pR","mGND","mGND",parasubs)[3]],
    t=0..20, refine=1, title= "Center of Left Trailer Tire", labels= ["time", "Z
    (meters)"],axes=BOXED);
>plots[odeplot](SolnXdot, [t,odeVars[9]*180/Pi], 0..10,numpoints=500,title= "Pendulum
    Angle vs time", labels= ["time", "Pendulum Angle (deg)"],axes=BOXED);
>plots[odeplot](SolnXdot, [t,GetFrameMotion("r","pR","mGND","mGND",parasubs)[3]]
    ,t=0..20, refine=1, title= "Center of Left Trailer Tire", labels= ["time", "Z
    (meters)"],axes=BOXED);
>plots[odeplot](SolnXdot,[GetFrameMotion("r","pR","cgC","cgC",parasubs)[2],GetFram
    eMotion("r","pR","cgC","cgC",parasubs)[3]] ,t=0..30, refine=1, title= "Coupler
    curve for point s1", labels= ["time", "theta y"],axes=BOXED);
> zPen(t):= GetFrameMotion("r","cgPen","mGND","mGND",parasubs)[3];
> zC(t):= GetFrameMotion("r","cgPen","cgC","cgC",parasubs)[3];
> yC(t):= GetFrameMotion("r","cgPen","cgC","cgC",parasubs)[2];
>plots[odeplot](SolnXdot,[eval(yPen(t)),eval(zPen(t))],t=0..5,numpoints=500,scaling=co
    nstrained);
>plots[odeplot](SolnXdot,[eval(yC(t)),eval(zC(t))],t=0..5,numpoints=500,scaling=constra
    ined);
> eval(zC(t),[theta_C(t)=rhs(SolnXdot(0)[9]),theta_Pnu(t)=rhs(SolnXdot(0)[8]]);
> z:=SolnXdot(t)[11];

```

```

>yC_step:=eval(yC(t),[theta_Pen(t)=thetaPen_step,theta_C(t)=thetaC_step,theta_Pnu(t)
    thetaPnu_step]);
> a:=eval(GetFrameMotion("r","pL","mGND","mGND",parasubs));
> ressort:=proc(ix,iy,fx,fy,n,lu,cl,t)
local i,p,dx,dy,lm,beta,cosalpha,sinalpha,k,h,ssomm,csomm,sdiff,cdiff,x,y,c;
dx:=(fx-ix)/n;
dy:=(fy-iy)/n;
lm:=(sqrt((fx-ix)^2+(fy-iy)^2))/n;beta:=arccos(lm/(4*lu));
cosalpha:= dx/lm; sinalpha:= dy/lm;
k:= cos(beta); h:=sin(beta);
ssomm:= sinalpha*k+cosalpha*h;sdiff:=cosalpha*h-sinalpha*k;
csomm:=cosalpha*k-sinalpha*h;cdiff:=cosalpha*k+sinalpha*h;
p[0]:= plot([[ix, iy],[ix+dx,iy+dy]], color=cl,thickness=t);
for i from 1 to n-2 do
x:= ix+(dx*i); y:= iy+(dy*i);
p[i]:=plot([[x,y],[x+lu*csomm,y+lu*ssomm],[x+dx/2,y+dy/2],[x+dx/2+lu*cdiff,y+dy/2-
    lu*sdiff],[x+dx,y+dy]], color=cl,thickness=t);
od;
p[n-1]:=plot([[ix+dx*(n-1),iy+dy*(n-1)],[fx,fy]],color=cl,thickness=t);
p:= plots[display](seq(p[i], i=0..n-1));
end:
> cordinate:=proc(point,time)
local v1,v2,v3,v4,v5,cord;
v1:= rhs(SolnXdot(time)[7]);
v2:= rhs(SolnXdot(time)[8]);
v3:= rhs(SolnXdot(time)[9]);
v4:=rhs(SolnXdot(time)[10]);
v5:=rhs(SolnXdot(time)[11]);
cord:=eval(GetFrameMotion("r",point,"mGND","mGND",parasubs),[s_H(t)=v1,theta_Ci
    t(t)=v2,theta_H(t)=v3,theta_V(t)=v4,theta_pnu(t)=v5]);
end:

```

```

> cordinate("cgC",0);
> with(plottools);
> anim:=proc(timeI,time,n)
local i,r1,r2,r3,r4,frame,step,c,l,lpen,cpen,gnd,cH,cV,IH,IV;
gnd:=line([-2,0],[2,0],colour=black,thickness=4);
step:=1/n;
for i from timeI*n to time*n do
c[i] := ellipse([cordinate("n47",i*step)[2],cordinate("n47",i*step)[3]],1.2,0.6095,
filled=true,color=blue,thickness=2):
l[i]:=line([cordinate("pL",i*step)[2],cordinate("pL",i*step)[3]],[cordinate("pR",i*step)[2]
,cordinate("pR",i*step)[3]], color=black,thickness=2):
lpen[i]:=line([cordinate("PV",i*step)[2],cordinate("PV",i*step)[3]],[cordinate("cgPen",i*
step)[2],cordinate("cgPen",i*step)[3]], color=red,thickness=2):
cpen[i] := circle([cordinate("cgPen",i*step)[2],cordinate("cgPen",i*step)[3]], 0.1,
color=green,thickness=2):
cV[i]:=circle([cordinate("PV",i*step)[2],cordinate("PV",i*step)[3]],0.02,
color=black,thickness=2):
cH[i]:=circle([cordinate("pH",i*step)[2],cordinate("pH",i*step)[3]],0.02,
color=black,thickness=2):
IH[i]:=line([cordinate("pH",i*step)[2],cordinate("pH",i*step)[3]],[cordinate("n47",i*step)
[2],cordinate("n47",i*step)[3]], color=black,thickness=1):
IV[i]:=line([cordinate("PV",i*step)[2],cordinate("PV",i*step)[3]],[cordinate("n47",i*step
)[2],cordinate("n47",i*step)[3]], color=black,thickness=1):
frame[i]:= display( {gnd,c[i],l[i],lpen[i],cpen[i],cV[i],cH[i],IH[i],IV[i]});
od:
display([seq(frame[i],i=timeI*n..time*n)],insequence=true,scaling=constrained,axes=non
e);
end:
> anim(20,30,1);

```

### [3] Code for 3-D Trailer Model

```
> restart;
> with(DynaFlexPro);with(plots);
      "DynaFlexPro - version 2.4.0"
      "Copyright 2005-2007, MotionPro Inc."
      "`DynaFlexPro Tire` components installed.
      "Type '?DynaFlexPro' for help with DynaFlexPro."
>Model:=BuildEQs("D:/Travail/VENU_GORU/examples/project/2dPnuTrammel.dfp",["
      DynSimpType","Simplify"]);
      "Analyzing system..."
      "Performing constraint analysis..."
      "The system has 3 degree(s) of freedom. It is modeled using 5 generalized
      "Dynamic analysis complete."

      "Saving model for future use...: "
> with(Model);GetParams();
> parasubs:=[Clat=100000, Clong=100000, Crr=0,r2=0.572/2, G=9.81,mu1=1, mu2=1,
f=0.66,
Ixxc=5000*f,
Ixxp=(750+2*n3*30),
tp=1.05,hr3=0.24,hp=0.3, ps3=1.285-hr3,
R=0.5,
K_Roue=870000,D_Roue=100000,
KSusp3=1800000,Krot3=850000,
DSusp3=350000,Drot3=35000*3,
```

```

m_Cit=5000*f,
m_Susp3=908+400,
n2=4,n3=4,
a=2.4/2,b=1.219/2,fill=1,pa=0.7396,liquidfull=22000,
hFill=fill*2*b,
ti=19,
#Trammel Pendulum Parameters @ 50%,
hFix = 0.0727383943-hp,
m_Fix = 2801.344824*f,
m_pen = 8198.65516*f,
abar = 0.634381521,
bbar = 0.3222129477,
mtot = 11000*f,
IxxPen=1,IyyPen=1,IzzPen=1,
IxxFix=m_Fix/mtot*18300,IyyFix=m_Fix/mtot*183000,IzzFix=m_Fix/mtot*183000,H=
1.555,
#F=piecewise(t<ti,0.04*G*t,t>=ti,0.04*G*ti)
F=0.36*G*sin(2*Pi*t/3)
];
> BuildSimCode(Model,{"Xdot"},"MapleProc","Optimize",[op(parasubs)]);
> odeVars := convert(convert([Model:-vX],Vector),list);
> ICs:=array([0,0,0,0,0,0,0,0,0]);
> tr := time():
SolnXdot:= dsolve(numeric, implicit=false, procedure=pXdot, abserr = 1e-8, relerr=1e7,
start=0, initial=ICs, output=listprocedure, procvars= odeVars, range=0..50):
Time_to_integrate := time()-tr;
> plots[odeplot](SolnXdot, [t,GetFrameMotion("r","pR","mGND","mGND",parasubs)[3]]
,t=0..20, refine=1, title= "Center of Left Trailer Tire", labels= ["time", "Z
(meters)"],axes=BOXED);

```

```

> plots[odeplot](SolnXdot, [t,odeVars[9]*180/Pi], 0..10,numpoints=500,title=
  "Pendulum Angle vs time", labels= ["time", "Pendulum Angle
  (deg)"],axes=BOXED);
>plots[odeplot](SolnXdot, [t,GetFrameMotion("r","pR","mGND","mGND",parasubs)[3]]
  ,t=0..20, refine=1, title= "Center of Left Trailer Tire", labels= ["time", "Z
  (meters)"],axes=BOXED);
>plots[odeplot](SolnXdot,GetFrameMotion("r","pR","cgC","cgC",parasubs)[2],GetFram
  eMotion("r","pR","cgC","cgC",parasubs)[3]] ,t=0..30, refine=1, title= "Coupler
  curve for point s1", labels= ["time", "theta y"],axes=BOXED);
> zPen(t):= GetFrameMotion("r","cgPen","mGND","mGND",parasubs)[3];
> zC(t):= GetFrameMotion("r","cgPen","cgC","cgC",parasubs)[3];
>plots[odeplot](SolnXdot,[eval(yPen(t)),eval(zPen(t))],t=0..5,numpoints=500,scaling=co
  nstrained);
>plots[odeplot](SolnXdot,[eval(yC(t)),eval(zC(t))],t=0..5,numpoints=500,scaling=constra
  ined);
> eval(zC(t),[theta_C(t)=rhs(SolnXdot(0)[9]),theta_Pnu(t)=rhs(SolnXdot(0)[8])]);
> z:=SolnXdot(t)[11];
>yC_step:=eval(yC(t),[theta_Pen(t)=thetaPen_step,theta_C(t)=thetaC_step,theta_Pnu(t)=
  thetaPnu_step]);
> a:=eval(GetFrameMotion("r","pL","mGND","mGND",parasubs));
> ressort:=proc(ix,iy,fx,fy,n,lu,cl,t)
local i,p,dx,dy,lm,beta,cosalpha,sinalpha,k,h,ssomm,csomm,sdiff,cdiff,x,y,c;
dx:=(fx-ix)/n;
dy:=(fy-iy)/n;
lm:=(sqrt((fx-ix)^2+(fy-iy)^2))/n;beta:=arccos(lm/(4*lu));
cosalpha:= dx/lm; sinalpha:= dy/lm;
k:= cos(beta); h:=sin(beta);
ssomm:= sinalpha*k+cosalpha*h;sdiff:=cosalpha*h-sinalpha*k;
csomm:=cosalpha*k-sinalpha*h;cdiff:=cosalpha*k+sinalpha*h;
p[0]:= plot([[ix, iy],[ix+dx,iy+dy]], color=cl,thickness=t);
for i from 1 to n-2 do

```



```

x:= ix+(dx*i); y:= iy+(dy*i);
p[i]:=plot([[x,y],[x+lu*csomm,y+lu*ssomm],[x+dx/2,y+dy/2],[x+dx/2+lu*cdiff,y+dy/2-
lu*sdiff],[x+dx,y+dy]], color=cl,thickness=t);
od;
p[n-1]:=plot([[ix+dx*(n-1),iy+dy*(n-1)],[fx,fy]],color=cl,thickness=t);
p:= plots[display](seq(p[i], i=0..n-1));
end:
> SolnXdot(time);
> cordinate:=proc(point,time)
local v1,v2,v3,v4,v5,cord;
v1:= rhs(SolnXdot(time)[7]):
v2:= rhs(SolnXdot(time)[8]):
v3:= rhs(SolnXdot(time)[9]):
v4:=rhs(SolnXdot(time)[10]):
v5:=rhs(SolnXdot(time)[11]):
cord:=eval(GetFrameMotion("r",point,"mGND","mGND",parasubs),[s_H(t)=v1,theta_Ci
t(t)=v2,theta_H(t)=v3,theta_V(t)=v4,theta_pnu(t)=v5]);
end:
> cordinate("cgC",0);
> with(plottools);
> anim:=proc(timeI,time,n)
local i,r1,r2,r3,r4,frame,step,c,l,lpen,cpen,gnd,cH,cV,lH,lV;
gnd:=line([-2,0],[2,0],colour=black,thickness=4);
step:=1/n;
for i from timeI*n to time*n do
c[i] := ellipse([cordinate("n47",i*step)[2],cordinate("n47",i*step)[3]],1.2,0.6095,
filled=true,color=blue,thickness=2):
l[i]:=line([cordinate("pL",i*step)[2],cordinate("pL",i*step)[3]],[cordinate("pR",i*step)[2]
,cordinate("pR",i*step)[3]], color=black,thickness=2):
lpen[i]:=line([cordinate("PV",i*step)[2],cordinate("PV",i*step)[3]],[cordinate("cgPen",i*
step)[2],cordinate("cgPen",i*step)[3]], color=red,thickness=2):

```

```

cpen[i] := circle([coordinate("cgPen",i*step)[2],coordinate("cgPen",i*step)[3]], 0.1,
    color=green,thickness=2):
cV[i]:=circle([coordinate("PV",i*step)[2],coordinate("PV",i*step)[3]],0.02,color=black,thic
    kness=2):
cH[i]:=circle([coordinate("pH",i*step)[2],coordinate("pH",i*step)[3]],0.02,color=black,thic
    kness=2):
IH[i]:=line([coordinate("pH",i*step)[2],coordinate("pH",i*step)[3]],[coordinate("n47",i*step)
    [2],coordinate("n47",i*step)[3]], color=black,thickness=1):
IV[i]:=line([coordinate("PV",i*step)[2],coordinate("PV",i*step)[3]],[coordinate("n47",i*step
    )[2],coordinate("n47",i*step)[3]], color=black,thickness=1):
frame[i]:= display( {gnd,c[i],l[i],lpen[i],cpen[i],cV[i],cH[i],IH[i],IV[i]});
od:
display([seq(frame[i],i=timeI*n..time*n)],insequence=true,scaling=constrained,axes=non
    e);
end:
> anim(20,30,1);

```

#### [4] Code for Calculation of Trammel Pendulum Parameters

```

> restart;
> a:=2.4/2;b:=1.219/2;fill:=1;liquidfull:=22000;
> hFill:=fill*2*b;
> bbar:=b*(1+(- 1.780896+1.542048*b/a)*fill +(0.7726259-1.304727*b/a)*(fill)^2);
> abar:=a/b*bbar;
> xh:=a*(2*hFill/b-(hFill/b)^2)^0.5;
> #Trammel Pendulum Parameters,
> f:=2*a*(2*y/b-(y/b)^2)^ 0.5;
> ycg:=1/Ah*int(y*f,y=0..hFill);
> mtot:=Ah/Pi/a/b*liquidfull;
> m_pen:=mtot*(1+(-
0.863+1.237*ln(a/b))*0.5*hFill/b(0.1226+1.2489*ln(a/b))*(0.5*hFill/b )^2);

```

```

> m_Fix:=mtot-m_pen;
> hFix1:=(ycg-m_pen/mtot*b*(1-bbar/b))/(1-m_pen/mtot);
> hFix:=b-hFix1;
> hFix1/b;
m_pen/mtot;
bbar/b;

```

## **[5] Trammel Pendulum Parameters at different fill levels**

```

> #Trammel Pendulum Parameters @ 10,
hFix = -0.4811001390-hp,
m_Fix = 13.95425150,
m_pen = 1131.014174,
abar = 1.081599505,
bbar = 0.5493624154,
mtot = 1144.968425,
> #Trammel Pendulum Parameters @ 30,
hFix = 0.0268816267-hp,
m_Fix = 525.5719985,
m_pen = 5025.375329,
abar = 0.8527137142,
bbar = 0.4331075074,
mtot = 5550.947328,
> #Trammel Pendulum Parameters @ 50%,
hFix = 0.0727383943-hp,
m_Fix = 2801.344824,
m_pen = 8198.65516,
abar = 0.634381521,
bbar = 0.3222129477,
mtot = 11000,
> #Trammel Pendulum Parameters @ 70%,
hFix = 0.0470126789-hp,

```

```
m_Fix = 8095.337120,  
m_pen = 8353.715534,  
abar = 0.426602926,  
bbar = 0.2166787363,  
mtot = 16449.05265,  
> #Trammel Pendulum Parameters @ 90%,  
hFix = 0.0086720730-hp,  
m_Fix = 16832.44350,  
m_pen = 4022.588066,  
abar = 0.2293779290,  
bbar = 0.1165048731,  
mtot = 20855.03156,  
> #Trammel Pendulum Parameters @ 100%,  
hFix = -0.0004364970-hp,  
m_Fix = 21860.55323,  
m_pen = 139.4467646,  
abar = 0.1347230295,  
bbar = 0.06842807210,  
mtot = 21999.99999,
```